SUPPORTED LIPID BILAYER ELECTROPHORESIS: A NEW PARADIGM IN MEMBRANE BIOPHYSICS AND SEPARATIONS

A Dissertation

by

HUDSON PALMER PACE

Submitted to the Office of Graduate Studies of
Texas A&M University
in partial fulfillment of the requirements for the degree of

DOCTOR OF PHILOSOPHY

Approved by:

Chair of Committee,	Paul S. Cremer
Committee Members,	David H. Russell
	Siegfried Musser
	David P. Barondeau
Head of Department,	David H. Russell

December 2012

Major Subject: Chemistry

ABSTRACT

The motivation of this work was to produce novel analytical techniques capable of probing the physical properties of the cell surface. Many researchers have used supported lipid bilayers (SLBs) as models to study the structure and function of the cell membrane. The complexity of these models is consistently increasing in order to better understand the myriad of physiologically relevant processes regulated by this surface. In order to aid researchers in studying such phenomenon, the following contributions were made.

To manipulate components within the cell membrane, an electrophoretic flow cell was designed which can be used as a probe to study the effect of electrical fields on charged membrane components and for the separation of these components. This devise allows for the strict control of pH and ionic strength as species are observed in real-time using fluorescence microscopy. Additionally, advancements have been made to the production of patterned heterogeneous SLBs for use in separations and to probe the interactions of membrane components. The methodology to couple SLB separations and matrix-assisted laser desorption ionization mass spectrometry (MALDI-MS) imaging was devised. This technology allows for the label-free mapping of the SLB surface post electrophoresis in order to observe naturally occurring species unperturbed by the addition of extrinsic tags. The final contribution, and perhaps the greatest, is the development of a procedure to create highly mobile SLBs from native membranes. These surfaces have vast potential in that they are no longer simple models of the cell

surface, they are in fact the actual cell surface made planar. This advancement will be of great use to biophysicists and biochemists interested in using surface specific analytical methods to better understand physiological processes. These highly mobile native membrane surfaces have been coupled with the SLB electrophoresis technology to separate discrete bands of lipids and proteins, a proof of principle that will hopefully be further developed into a standard method for membrane proteomic studies.

Collectively the tools and methodologies described herein show great potential in allowing researchers to further add to mankind's understanding of the cellular membrane.

DEDICATION

The last 5 years have been quite the journey and while the destination is all that I had ever hoped for, it was the path to this point that I will remember more than the day the accomplishment finally was rewarded to me. Earning a Ph.D. is an experience like no other, the roller coaster of emotions is almost an induced form of manic depression. The high of success coupled with crippling defeats on almost a weekly basis tests ones resolve and often times pushes you to the edge of insanity.

The journey has been tolerable through the support of my family and friends. You have perked me up on dark days and kept me grounded when my head swells to the point that I could drift away. It is for these reasons that this tomb of knowledge is dedicated to all of you.

ACKNOWLEDGEMENTS

I would like to thank Paul Cremer for giving me the opportunity to be part of his research group and for his consistent encouragement. Your enthusiasm for science is addicting and I am glad I get to call you my academic father. You kept me focused when it was needed while allowing independence for me to grow as a scientist. I also greatly appreciate the mentorship of Dr. David Russell during my time as a pseudo member of your group. You allowed me the freedom to explore the amazing world of imaging mass spectrometry, which will forever remain an area of intrigue for me. Dr. Musser you have always kept me on my toes with your inquisitive questions and I am glad that I have had a chance to collaborate with you on what I consider to be some of my most intriguing work thus far. Our collaboration has sparked the desire to pursue a career in membrane protein studies. Last but not least, Dr. Barondeau you have been a warm smile in the hallways and ever since I first met you during the orientation mixer, which seems like a lifetime ago, you have had a calming effect on me; which is why I choose you for my committee.

As in any arduous journey, a bond has been forged between the peers whom I have shared this path with. Mike, I could not have asked for a better roommate during my years in grad school. Aaron, you always made work a more enjoyable environment and I could not have asked for a better coworker. Both of you have been great council through the difficult times and I hope that wherever our paths post grad school take us,

we will keep in touch and remain close for the rest of our lives. More than anyone else, I feel I owe my sanity and survival of this program to having you both as best friends.

My family has always supported me and showered me with love that keeps my batteries charged and ready to take on whatever life has in store for me. A special thanks to my parents: Sue Albin, Jerry Pace, and Doris Pace. Thank you for providing the opportunities that have allowed me to accomplish so much. Also a special thanks to my sister for being a dependable consigliere over the years, one I hope to have for the rest of my life. I know that no matter what physical distance we may find between us, we will always be close in each other's hearts and minds.

Of course a special thanks to Jen, the best girlfriend a guy could ask for! You have helped me overcome so many obstacles in the short time we have been together and you continue to make me a better person with each passing day. You will forever have my love and respect. I can only hope to fulfill the potential you see in me.

TABLE OF CONTENTS

Page

LIST OF FIGURES

Page

LIST OF TABLES

Page

CHAPTER I

INTRODUCTION

During the last decade there has been dramatic growth in interdisciplinary research. Indeed, the lines that once divided disciplines seem to dissolve more with each passing year. It is at these emerging interfaces where a young enthusiastic scientist has the greatest chance to make a name for himself, not because he is smarter than those that came before, but because more resources are readily accessible allowing for the intermingling of orthogonal literature and knowledge in order to make discoveries and draw connections that were previously too obscure.

Biological surface science is one of these emerging fields. It has made bed fellows of analytical method development, material science, molecular biology, and physics, just to name a few. The offspring of these collaborations have been applications based (e.g., biosensors, implant coatings, etc.) as well as tools for researchers to better understand the fundamentals of biological systems. While this field is only still emerging, it has spawned a great diversity of research areas already with nearly limitless growth potential. The cell membrane is arguably one of the most complex biological surfaces known. Expeditions into understanding its structure and function are the driving force behind the research discussed in this dissertation. Indeed, the breakthroughs described herein were motivated by the desire to build tools that biochemists and biophysicists could utilize to elucidate fundamental knowledge about the cell surface.

The cellular membrane is truly a marvel of natural engineering when considering the degree of versatility required to regulate the interactions between the cell and its environment. In order to accomplish this feat a great diversity of lipid and protein species are utilized. Understanding the interactions of these various components, their structure and their effect on the physiology of the cell is of great importance to researchers trying to understand mechanisms of disease.

Great strides have been made in the analysis of the lipid components of the cell membrane and their physiological roles due to their robust nature and high miscibility in organic solvents.[1] However, analyses of the protein components of the membrane have been hindered due to the amphipathic nature of a subset of this population. Shotgun proteomic methods and 2-dimensional electrophoresis coupled with mass spectrometry have vastly enhanced our understanding of the water-soluble proteins of the cell, but there have been problems investigating the membrane protein population.[2-5] Integral membrane protein purification, identification, and characterization using traditional proteomics methods are hindered due to their hydrophobicity and alkaline isoelectric points.[2] The detergents required for the extraction and solubilization of these species often interfere with analysis methods downstream. Attempts to minimize this often result in protein denaturation, aggregation, and loss of analyte.[3] Since membrane proteins compose 70% of current drug targets, drug discovery initiatives are very interested in increasing the body of knowledge associated with these elusive species.[5] It has been proposed that separation, purification, and analysis of membrane proteins within their

native phospholipid bilayer environment would allow better understanding of their native structure and abundance.

Supported phospholipid bilayers (SLBs) have been used extensively to study the chemistry of the cell surface.[6-10] While most of these studies investigate lipid systems, reports of membrane proteins in SLBs do appear in the literature.[11-16] While issues with denaturation of membrane proteins on the solid support have been reported, many innovative ideas, such as polymer cushions, have emerged to resolve this issue.[13,15,17] Solving the mobility issues associated with protein incorporation has enhanced the legitimacy of using SLBs as a model for the native membrane.

Sackmann pioneered electrophoretic manipulation of membrane components within SLB systems. It was shown that oppositely charged fluorescently labeled lipids would migrate in different directions in an electric field.[18] Groves and Boxer soon after showed that it was possible to create a concentration gradient of a charged fluorescently labeled lipid against a physical barrier.[19] It was later shown that the migration of membrane-tethered proteins within an electric field could produce a concentration gradient against a physical barrier.[20] Several years later the creation of physical barriers in the SLB after formation of a concentration gradient allowed for the permanent separation of oppositely charged lipids.[21] While each of these accomplishments in SLB separations were important stepping stones and proofs of principle, there was still quite the void between the reported technology and the suggestion that this technology could be developed to separate components from native membranes.

In 2007, Cremer and coworkers produced the most convincing proof that SLBs could be exploited for high resolution electrophoretic separations of membrane-bound components when they separated three negatively charged lipids from each other to base line resolution, two of which were isomers.[22] This was accomplished by changing the separation setup such that the material to be separated was confined to a sharp band within the SLB prior to electrophoresis unlike the homogeneous SLBs that were used in previous studies. In addition, the incorporation of cholesterol into the separation region of the SLB attenuated the lateral diffusion of the components during their electrophoretic migration producing a high resolution separation.

While electrophoretic separation of lipids can be accomplished without the need for buffered system with strict pH control, advancements were needed in order to achieve the next step in the manipulation of membrane proteins. Chapter III reports on our endeavor to produce a new electrophoresis device, which effectively controls pH and removes the products of electrolysis so that electrophoresis can be performed under buffering conditions.[23] Within this report, we show the minor effect pH and ionic strength changes have on lipid electrophoretic mobility as well as the significant effect these parameters have on the electrophoretic mobility of peripheral membrane proteins. The advancements of this work take another large step towards the end goal of separation and purification of proteins from native membranes in order to produce a new technology for membrane proteomics.

Since this new method of separation would ideally yield membrane species in their native conformation, a label free detection method would be advantageous.

Currently the investigations of membrane species migration in SLB systems utilize fluorescent microscopy. While fluorescence microscopy has a very low limit of detection, it is dependent upon the conjugation of a fluorescent tag to the analyte. Conjugation of fluorescent tags to molecules can alter their structure, function, and can affect their behavior in the membrane.[24] Additionally, there is also a finite number of fluorophore tags available indicating that there is a limitation to the number of analytes that can be detected within a single sample without ambiguity due to spectral overlap.

Chapter IV reports on the use of matrix-assisted laser desorption/ionization time-of-flight (MALDI-TOF) MS imaging for visualizing the presence of membrane components post electrophoretic separation. This technology proved to be useful for visualizing non-fluorescently labeled naturally occurring membrane receptors. The methodology developed herein holds great promise for use in the analysis of future SLB separations. At the risk of sounding overly philosophical, we only know that which our senses can tell us and thus we are too often slaves to the limited observations we have available to draw conclusions from. This technology can only enlighten us.

Chapter V is the crowning achievement of the work presented herein. The long prophesized goal of separating out membrane proteins from native membranes has been accomplished! What seemed like an impossible feat 5 years ago, when all we had accomplished was the separation of a few synthetic lipids, has been attained. Within this chapter the methodology to produce highly mobile SLBs from the inverted inner membrane vesicles of *E. coli*, fractionate them electrophoretically, and then visualize the membrane proteins present using a pseudo-Western blot procedure is described. While

the results contained in this chapter are only a proof of principle, the most difficult problems have been solved and upon further development the methods contained herein will blaze new paths for membrane proteomics studies as well as provide a valuable tool to biophysicists and biochemists.

CHAPTER II

EXPERIMENTAL METHODS BACKGROUND

This chapter is a presentation and discussion of a few of the methods that were adapted to accomplish the research discussed in this dissertation.

Creating Patterned Supported Lipid Bilayers

While there are several procedures available to create SLBs, the simplest is vesicle fusion. Vesicle fusion historically has been limited to small unilaminar vesicles that contain a relatively narrow selection of lipid species. Upon joining the group, the art of scratching a SLB with a pair of tweezers was part of basic training. Ideally, only the bilayer sitting 1 nm from the surface is damaged and not the substrate itself. This was an important skill for creating the origins needed for high resolution SLB electrophoresis. A change was needed.

While many methods have been reported for patterning SLBs, none seemed to have the combination of ease of use and quality desired.[9] It was during the period in which MALDI-MS imaging of SLBs post separation were being investigated that a wider origin, than traditionally attained with a pair of tweezers, was required. Since tweezers often produced origins on the order of ~100 μm wide and the laser spot for MALDI-MS was ~100 μm wide, the limits of spatial resolution for the MS imaging experiments was being pushed. Attempts at using wider tipped tweezers for making origins produced striated patterns, loving referred to as multi-lane highways. Thus, the

origin was actually a mixture of analyte vesicles and the separation SLB lipids. In order to produce an origin with a higher purity of analyte vesicles, polydimethylsiloxane (PDMS) stamps were utilized. This polymer could be cut into various sizes and used to create a very uniform, high purity origin; ideal for MS imaging. Additionally, it was discovered that the sharp interface at the perimeter of a stamped origin can be used to concentrate analytes as they pass from a less viscous (no cholesterol) SLB into the highly viscous (25 mol% cholesterol) separation SLB, as discussed in Chapter IV.

Cleaning and Labeling *E. coli* Inner Membrane Vesicles

The *E. coli* inverted inner membrane vesicles (IMVs) received from Dr. Musser's lab had been freshly inverted, via a French press, and contained a mixture of buffers and media components. It was important to perform a buffer exchange on the IMV solution in order to better understand the composition of the samples for future analysis. For conjugating a dye to the IMV material, the appropriate buffer for that conjugation reaction must be used (e.g., no Tris buffer if you are labeling amines).

In the following protocol Phosphate Buffered Saline (PBS) was utilized for labeling the IMVs with a succinimidyl ester, TFP ester, or SDP ester containing Alexa Fluor dye. These dyes label free amines (mostly 1° and some 2° amines). Since the major lipid component of *E. coli* is phosphatidylethanolamine (which contains a 1° amine), this lipid competes with the proteins for conjugation. A maleimide or haloalkyl containing dye could be used to conjugate thiol groups in order to more selectively label proteins (as no lipids contain thiols); however, reduction of the thiols (breaking of

disulfide bonds) is often used to increase labeling efficiency and this reduction can lead to breaking up of protein complexes held together by disulfide bonds.

Cleanliness is important when processing the IMVs. A 0.2 μm syringe filter from Millipore (Bedford, MA) was utilized for sterilizing all buffers coming into contact with the IMVs. Many filters (e.g, syringe filters and molecular weight cut-off filters) use sodium azide to prevent bacterial growth during storage. The azide will compete with proteins for reaction with the amine-labeling dye. Thus, the first several rinses through a new filter were disposed of before collection of stock filtered buffers. The two buffers used in this protocol are Tris Buffered Saline (TBS: 10 mM Tris, 100 mM NaCl, pH 7.4) and PBS (10 mM Phosphate Buffer, 150 mM NaCl, pH 7.4).

Two ~5 M sucrose solutions were made for this procedure, one with each of the two buffers. Higher concentration sucrose produces a firmer cushion and creates a sharper interface for the IMVs to concentrate against, which increases the purity and yield of each step in the procedure. The solubility limit of sucrose in water at 25°C is 5.8 M. The sucrose solutions as well as all the buffers were kept at 4°C and the following procedure was carried out in the cold room at 4°C.

The first step of the labeling procedure was a buffer exchange to make sure that there were no free amines present other than those in the IMVs. Eight 1.5 mL centrifuge tubes received 0.3 mL of 5 M sucrose-PBS solution and then 0.2 mL of filtered PBS (no sucrose) was slowly added to the top. Two distinct layers were visible. Then, 0.4 mL of *E. coli* IMV solution was carefully pipetted into a centrifuge tube along with 0.4 mL of filtered PBS. The mixture was gently vortexed until homogenous and then carefully

pipetted onto the sucrose cushion. Great care was taken not to disturb the cushion. Filtered buffer additions were used to balance samples for centrifugation. Tubes were then centrifuged at 16,100 rcf (13,200 rpm) until the IMVs formed a sharp band at the interface of the two layers (~90 min).

Using a 0.2 mL pipette and a very steady hand, the IMV layer was removed with as little PBS and sucrose as possible. Some mixing at this stage was inevitable. If larger chunks of material were present, a 1 mL pipette was used to aid in collection; however, the collection was carried out with as small a volume as possible. When a decision had to be made, the top layer was chosen over collecting sucrose solution. The extracted IMV solution was then placed into another microcentrifuge tube along with the proper amount of buffer to bring the entire volume up to 0.8 mL (ideally less than 0.4 mL of IMV solution was collected and therefore at least 0.4 mL of fresh PBS was added). This mixture was gently vortexed to homogeneity, then pipetted gently into a tube containing a sucrose cushion. Great care was taken not to disturb the cushion. This buffer exchange was procedure was repeated another three times. Upon completion of the last buffer exchange, the extracted IMV solution was gently vortexed until homogeneous, and then either labeled or prepped for storage. The IMVs that were prepped for storage were mixed with glycerol to a final 40% v/v concentration and flash frozen with liquid nitrogen and stored at –80°C.

Labeling lysines is best done at a pH of 8.5 to 9.5, so 50 μL of 1 M bicarbonate buffer (pH 9) was added to 0.4 mL of IMV in order to hit the target pH range. This pH adjusted solution was then reacted with 0.5 mg of Alexa Fluor 594 carboxylic acid

succimidyl ester suspended in 25 μL of 200 proof ethanol. The reaction mixtures were gently vortexed at room temperature for 1 min every 10 min for an hour and then stored at 4°C overnight. The unconjugated dye and ethanol were removed by using the buffer exchange protocol outlined above, but with TBS in place of PBS. The Tris quenches any reactive dye still remaining. The buffer exchange process was repeated at least two rounds after the top layer appears completely clear (this usually meant 5-6 rounds of buffer exchange depending of the efficiency of IMV layer extraction).

Attempts at expediting this process through the use of molecular weight cut off filters seems to lead to low recoveries, probably because the membrane proteins stick to the membrane filter which is optimized for low adsorption of soluble proteins.

Preparation of Hybrid Vesicles

Glycerol in the sample has been observed to alter the optical density at 280 nm, thus it is suggested that the O.D. at 280 nm is taken at multiple dilutions. Upon correction for the dilution, the values attained from increasing dilutions will converge and reveal the accurate O.D. at 280 nm.

Once an accurate optical density at 280 nm of the IMV solution was calculated, adjust by either dilution or concentration to produce a stock with an O.D. at 280 nm of 4. This solution was then mixed 1:5 by volume with 0.5% PEG5Kce, 99.5% POPC. After vortexing, the solution was sonicated at 25°C for 2 hrs. The sample was removed from the sonicator and vortexed every 20 min and then the solution was shook to the bottom of the tube and returned to the sonicator. Samples were usually 50 μL total volume. This

procedure is still open for further optimization. Particularly, it would be ideal to lower the sonication time and temperature. Ideally a sonication procedure in which the sample was kept on ice and only exposed to sonication 10 s at a time would be nice, but these parameters have not been fully explored yet. It has been observed that glycerol increases the shelf life of the proteoliposomes and aids in the creation of continuous bilayers in the heterogeneous supported lipid bilayer system. It is advised to maintain a minimum of 10% glycerol in the proteoliposome solutions.

CHAPTER III

SUPPORTED BILAYER ELECTROPHORESIS UNDER CONTROLLED BUFFER CONDITIONS*

Introduction

The use of supported lipid bilayers (SLB) as model cell membranes is well-established.[7] There are multiple reports in the literature of attempts to use SLB-based techniques to investigate lipids, transmembrane proteins and membrane-associated proteins. There have been a number of significant successes in these efforts. In particular, the use of cushioned bilayers often results in a substantial fraction of the proteins in the membrane showing mobility by fluorescence recovery after photobleaching (FRAP) measurements.[12,13,25-28] Other techniques, such as surface acoustic wave generation and QCM-D, have been used to pattern and monitor lipids, lipid-bound proteins and membrane proteins.[29-31] Additionally, electrophoresis has shown promise as a method for separating charged membrane components in SLBs.[20,32-34] The motivation for these efforts stems in part from a desire to find new methods to separate membrane proteins in a lipid bilayer environment, rather than under harsher and more denaturing conditions.[2,35]

Early SLB electrophoresis moved or separated charged fluorescently labeled lipids.[18,19] In later reports, SLB-based separations were developed to the point that lipid

---

* Reprinted (adapted) with permission from Monson, C.F.; Pace, H.P.; Liu, C.; Cremer, P.S. *Anal. Chem.* **2011**, *83*, 2090. Copyright 2011 American Chemical Society.

molecules exhibiting only minor differences such as the ortho- and para- isomers of Texas Red 1,2-dihexadecanoyl-sn-glycero-3-phosphoethanolamine (TR-DHPE) could be separated.[22] Membrane-associated proteins have also been analyzed using SLB electrophoresis with some success. Groves et al.[20] first demonstrated that proteins covalently attached to lipids through a glycan-phophatidylinositol linkage could be moved electrophoretically on an SLB. More recently, a number of groups have reported the electrophoretic motion of proteins.[14,32-34] Of particular note, Han et al.[34] were able to control the electrophoretic motion of streptavidin bound to biotinylated lipids by varying the composition and thus the amount of charge in the bilayer.

When a potential is applied along an SLB, there are at least two possible mechanisms by which membrane-bound species may be transported. First is by the electrophoretic force. The magnitude of the electrophoretic force is a function of the charge on the molecule and the potential gradient. Thus, a difference in charge can be used to separate molecules. The second is the electroosmotic force. This is a byproduct of having a fixed charge, either on the glass substrate or on the bilayer itself. The fixed charge attracts counterions. When a potential is applied, the fixed charge remains stationary (or moves relatively slowly if in a bilayer), while the counterions migrate electrophoretically. This mass, directional movement of ions induces an electroosmotic flow, which can in turn exert a force on molecules that protrude above the plane of the bilayer (e.g., membrane proteins). Glass surfaces are negatively charged under most conditions, and thus the electroosmotic flow normally pushes material toward the cathode.[36]

In supported bilayer electrophoretic experiments, a potential is applied between two electrodes. This hydrolyzes water and generates protons and oxygen gas at the anode and hydroxide and hydrogen gas at the cathode. The SLB should therefore be isolated from these electrolysis products. In fact, the bubbles generated at an electrode can directly delaminate the SLB. Moreover, the pH swings induced by the electrogenerated ions can alter the electrophoretic mobility of pH-sensitive bilayer species. Proteins are particularly susceptible to pH changes due to the large number and variety of amino acids that can be protonated or deprotonated near physiological pH.

Traditionally, two strategies have been employed to minimize the effects of electrolysis. First, the experiment is performed with a high resistance between the two electrodes. This is done by constricting the aqueous volume above the bilayer and working at low ionic strength. This reduces the current that passes between the electrodes and thus the quantity of electrolysis products. It also reduces Joule heating, which can damage the SLB. A constricted solution volume additionally ensures that the majority of the potential drop occurs across the area of interest. Second, buffer reservoirs are placed around the electrodes in order to mitigate pH changes that result from the electrogenerated ions. The buffer is normally present only at low ionic strength (often 1 mM or less), but the relatively large volumes used provide some time-limited buffering capacity. This prevents large pH changes over the SLB until the buffering capacity of the reservoirs has been exhausted.

Combining thin volumes above the bilayers with larger reservoirs adjacent to it should allow the pH of the supported bilayer to remain relatively unchanged for several

minutes. This is sufficient to separate lipids, which generally have relatively high electrophoretic mobilities in SLBs. Membrane-associated proteins, on the other hand, can have lower mobilities. Thus, longer runs can be necessary to separate proteins. In order for the electrophoretic mobility of a protein to remain constant during an experiment, the pH must remain unchanged. Otherwise, the net charge on the protein will continuously be altered over the course of the experiment. Additionally, some proteins require relatively high ionic strength solutions to remain in their native state. These parameters are, unfortunately, incompatible with traditional SLB electrophoresis setups.

To enable longer electrophoretic runs at constant pH, we have developed a new flow cell (Figure 1). This device puts double channels on each side of a supported bilayer. The electrodes are embedded in the outer channels and buffer is flowed through both the inner and outer channels. This constant buffer flow ensures that the pH in the aqueous solution above the membrane remains within ±0.2 pH units of the initial pH (pH 3.3 to 9.3) at ionic strengths at or below 10 mM. As such, the apparatus enables electrophoresis experiments for indefinite time periods under controlled pH conditions. An additional benefit in these experiments is that higher ionic strengths can be employed than in previous setups. This is the case because the flowing solution constantly extracts heat generated by the electrodes. This setup was employed to monitor the electrophoretic mobility of Texas Red DHPE and streptavidin linked to the bilayer via biotin-PE. It was found that by altering the pH, the direction of travel of the streptavidin could be reversed.

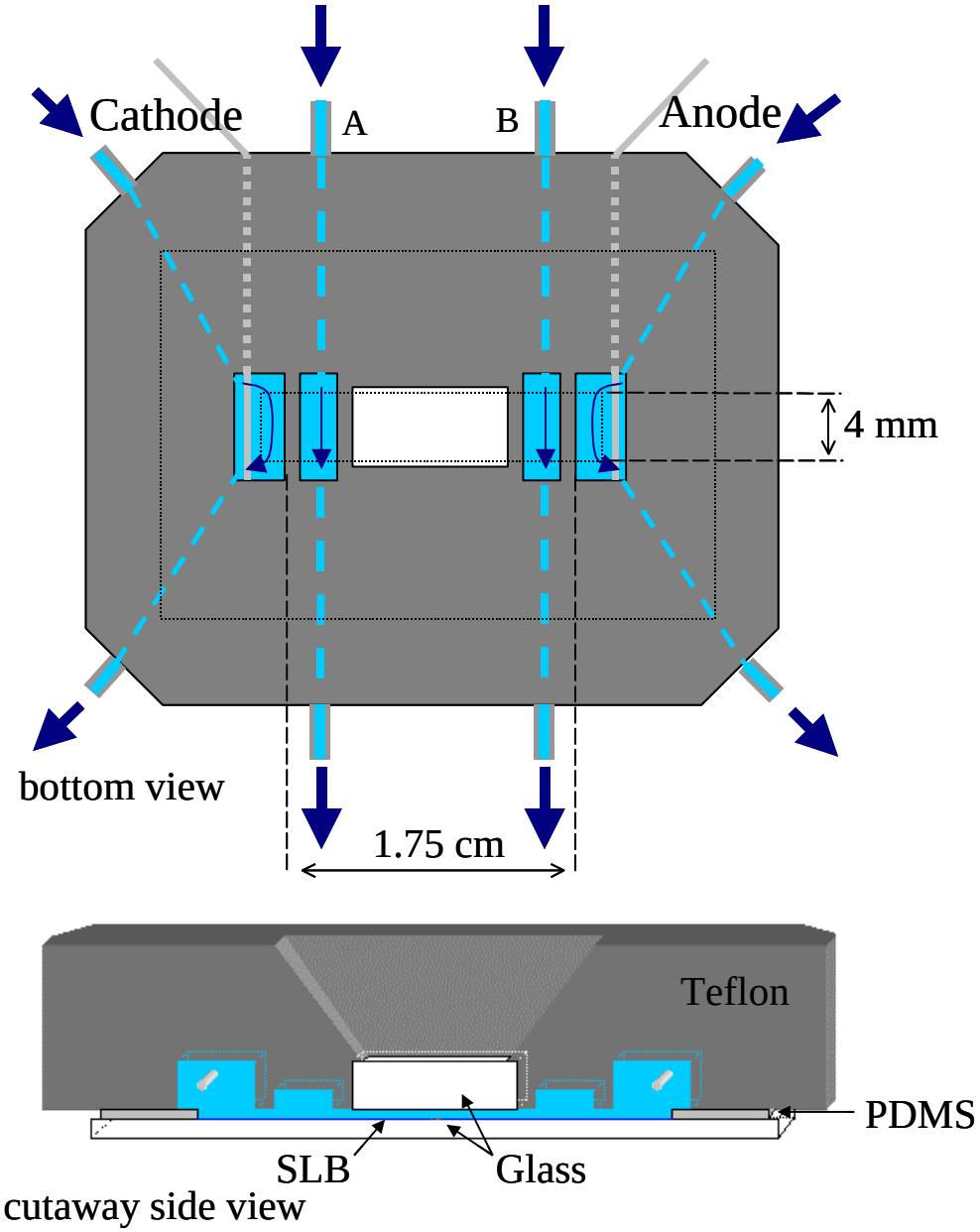

Figure 1. Schematic diagram of the flow cell designed for SLB electrophoresis. Buffer flows in tubes and holes (blue) in the Teflon into and out of 4 channels (Cathode, A, B, Anode) in the bottom face of the device. These channels clear electrolysis products generated by the electrodes (light gray lines) before they can reach the active area of the device holding the SLB components to be electrophoresed. The top schematic shows a view of the flow cell from below, while the bottom schematic shows a cutaway view.

Moreover, the electroosmotic contribution could be separately controlled by tuning the distance between the bilayer and the underlying support.

Experimental

Glass Cleaning. Glass coverslips (Corning, NY, 24x40 mm No. 1.5) were cleaned by boiling in 7X® solution (MP Biomedicals, Solon, OH) diluted 1:5 with distilled water. They were then rinsed thoroughly with purified water (Nanopure Ultrapure Water system, Barnstead) and blown dry with nitrogen. The coverslips were annealed at 530˚C for 5 hours and stored for up to two weeks before use.[37]

Vesicle Preparation. Vesicles were prepared via the freeze-thaw/extrusion method.[38,39] Lipids were mixed at the desired ratios in chloroform solutions. The chloroform was evaporated under a stream of nitrogen and the lipids were placed under vacuum for four hours to remove any remaining solvent. The lipid mixture was rehydrated with tris(hydroxymethyl)aminomethane buffer (10 mM Tris, 100 mM NaCl, pH 7.4, Tris/NaCl buffer) and subjected to ten freeze/thaw cycles in liquid nitrogen and warm water. The solution was extruded ten times through a track-etched polycarbonate membrane with 100 nm pores (Whatman), diluted to 1 mg/ml, and stored at 4˚ C until use. The average vesicle size of each batch of vesicles produced was found to be between 80 and 120 nm by dynamic light scattering using a 90Plus Particle Size Analyzer (Brookhaven Instrument Corp., Holtsville, NY).

SLB Formation. Supported lipid bilayers were formed via the vesicle fusion method as described previously.[6,21,40] A narrow line of analyte material could be added to the membrane by employing the scratch and backfill method (Figure 2).[22] To do this, an initial bilayer (shown in blue) was formed at the liquid/solid interface using a 1 mg/ml solution of 100 nm diameter vesicles within the confines of a polydimethylsiloxane (PDMS, Sylgard 184, Dow Corning, Midland, MI) well on a clean glass coverslip. The vesicles, which were made of 1-palmitoyl-2-oleoyl-sn-glycero-3-phosphocholine (POPC, Avanti Polar Lipids, Alabaster, AL), were incubated over the surface for at least 10 minutes before being washed away with fresh Tris buffer. These vesicles were doped with 0.5 mole percent C16 mPEG 5000 Ceramide (PEG, Avanti Polar Lipids, Alabaster, AL) in runs requiring a polymer cushion. Next, a solution containing the analyte vesicles was introduced above the surface and the surface was scratched with a Teflon-coated metal spatula as shown in Figure 2b. This removed a line of lipids and allowed the vesicles containing the analyte lipids to adsorb into the scratched area. Incubation of these vesicles was allowed to proceed for 8 minutes. After this, the slide was again rinsed with purified water followed by Tris/NaCl buffer. This produced a narrow band of labeled lipids, as illustrated in Figure 2c. This analyte band consisted of POPC doped with 1.0 mol% 1,2-dioleoyl-sn-glycero-3-phosphoethanolamine-N-(cap biotinyl) (b-DOPE, Avanti Polar Lipids, Alabaster, AL) and 0.1 mol% TR-DHPE (Invitrogen, Carlsbad, CA). Streptavidin could be bound to the surface by incubating a Tris/NaCl solution containing 0.01 mg/mL labeled streptavidin over the surface for 10 to 20 minutes followed by rinsing away excess protein with Tris/NaCl buffer.

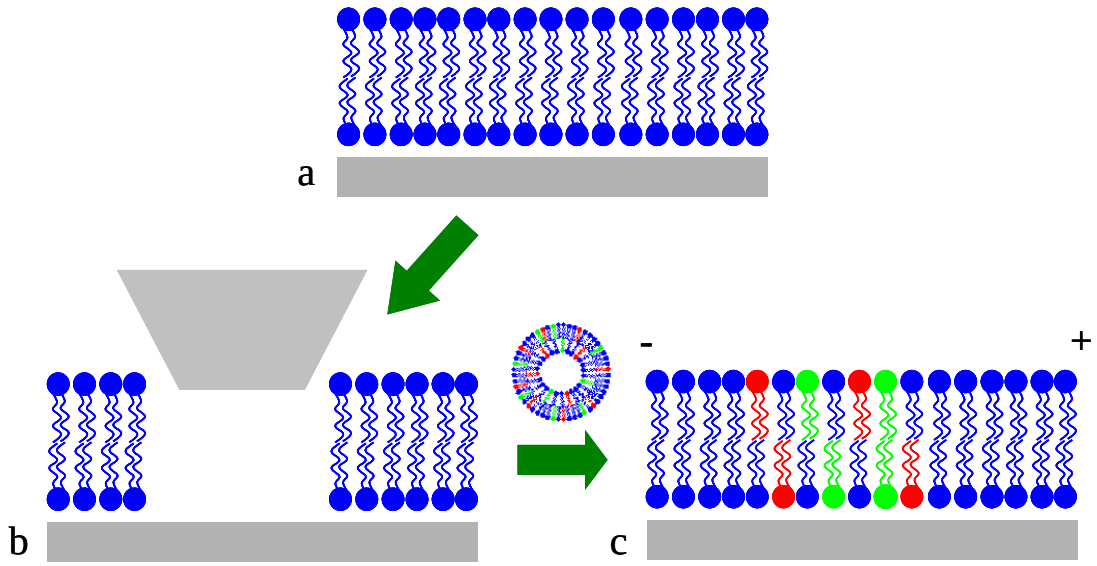

Figure 2. The scratch and backfill method of producing a band of lipids in a matrix for separations. (a) Vesicles are fused to a glass coverslip to form an SLB. (b) A Telfon-coated metal spatula is used to scratch the slide, removing a band of matrix material. (c) Vesicles containing a lipid mixture to be separated are then fused into the vacant area and a potential is applied along the bilayer.

Flow Cell. The electrophoresis flow cell setup (Figure 1) was manufactured in-house. It consisted of a Teflon body in which a series of channels, tubes, and a viewing window were machined. The SLB was held on a separate glass coverslip in a long, narrow well (20 mm by 4 mm) carved into a PDMS slab (30 mm x 20 mm x 0.1 mm). The coverslip/PDMS system was held tightly against the Teflon body by clamps. The two outer channels (labeled "Cathode" and "Anode" in Figure 1) were 1 mm deep and also held the platinum electrodes (0.25 mm diameter, shown in gray). The inner two channels (labeled "A" and "B" in Figure 1) were only 100 μm deep, which forced buffer to flow close to the coverslip supporting the bilayers. The inner channels ensured that any electrolysis products that escaped from the outer channels would be swept away before reaching the central region where the SLB was housed. Inlet and outlet buffer was carried by gravity in Teflon tubing to and from the device. A height difference of ~75 cm between the buffer reservoir and the device was employed to adjust the flow rate to ~0.6 ml per minute in each tube. It was found that the flow rate increased in a linear fashion with height. A 1 mm thick glass observation window was placed over the central region of the flow cell so that the bilayer could be visualized by fluorescence microscopy. This allowed the electrophoretic separation to be observed in real time using either an upright or an inverted microscope.

The PDMS well used in these experiments was fabricated by allowing PDMS to polymerize between two glass slides separated by the thickness of No. 1 coverslips (100-150 μm thick). A section of the PDMS sheet was cut out and removed to make the well. Thus, during an experimental run the SLB is held in a channel that is 100-150 μm high.

The PDMS well was rinsed with ethanol and purified water. Additional dust and particulates were removed with adhesive tape before it was affixed to the coverslip.

Streptavidin Labeling. Streptavidin with varying numbers of dye labels was used in this work. Unlabeled streptavidin was purchased from Sigma. A portion of this protein was labeled with 0.3 Alexa Fluor 488 dyes per molecule using a protein labeling kit (Molecular Probes, Carlsbad, CA). A second portion was labeled with 4.0 Alexa Fluor 488 dyes per protein also using the protein labeling kit. In all labeling experiments, the dye labeled protein was separated from unreacted dye molecules using a size exclusion column provided as part of the labeling kit with Tris/NaCl buffer as the eluent. The number of dyes per molecule was determined by measuring the UV/Vis absorbance of the labeled, purified streptavidin solution at 280 and 494 nm with an Agilent 8453 UV/Vis spectrometer. The degree of labeling was calculated as per the instructions in the protein labeling kit, using an extinction coefficient of 3.2 ml cm/mg for streptavidin.[41]

Results and Discussion

Flow Cell pH Control. In a first set of experiments, the pH in the four-channel flow cell was tested at a variety of values. The results are listed in Table 1. The outermost channels are designated “Cathode” and “Anode” as this is where the electrodes are housed. By contrast, the inner channels are designed “A” and “B”. As can be seen, solutions containing 1 mM of a buffering agent were used at 4 different pH values. In

the case of sodium citrate at pH 7.7, the salt was intentionally well outside of its buffering range to measure the pH variation in an essentially unbuffered solution. Under a final set of conditions, 10 mM and 100 mM NaCl were added, respectively, to 1 mM Tris buffer, which substantially increased the solution conductivity. In all cases, a 250 V (140 V/cm) potential was applied across the device and maintained for at least 30 minutes before the pH was measured in each of the four channels. A solution flow rate of 0.6 ml/min was constantly maintained in all channels. This meant that the flow velocity was actually an order of magnitude faster in the inner channels than in the outer channels. This faster flow rate in the inner channels actually kept the pressure higher there and forced a net solution flow from the inner channels to the outer channels. The control of electrolysis conditions by means of channel depth is similar in concept to work done in free-flow electrophoresis, which suffers from similar problems due to electrolysis products.[42]

Table 1. The Performance of the Flow Cell under Different Buffer and pH Conditions.[a]

Buffer	Initial pH	Buffer Capacity (mM/pH)	pH of Outlet Buffer			
			Cathode	A	B	Anode
1 mM Citrate	3.0	2.9	3.0	3.0	3.0	3.0
1 mM Citrate	5.2	0.62	5.3	5.2	5.2	5.1
1 mM Citrate	7.7	0.11	11.0	7.7	7.7	6.7
1 mM Tris	9.2	0.15	9.2	9.2	9.2	9.2
1 mM Tris 10 mM NaCl	7.4	0.34	9.0	7.5	7.3	3.3
1 mM Tris 100 mM NaCl	7.7	0.49	11.6	10.0	7.7	2.2

[a]Sodium was the cation in the citrate buffers.

As can be seen from Table 1, the pH of the inner channels never deviated within experimental error from the initial pH value of the solutions for all low ionic strength experiments. The outer channels showed more variances, especially in the cathode chamber for sodium citrate buffer at an initial pH of 7.7. As expected, substantial variance from the initial pH could also be seen in the anode and cathode chambers when 10 or 100 mM NaCl was added. Nevertheless, the two inner channels maintained pH values within 0.1 pH unit of the initial solution in the 10 mM case. Such a result ensured that the SLB chamber between these two channels would only be subjected to very small pH swings up to 10 mM ionic strength. Since a pH variation of ~2 pH units in the A channel was observed with 100 mM NaCl, salt concentrations were held to only 10 mM in all subsequent electrophoresis experiments with bilayers.

It should be noted that the flow of buffer through the device helped in two ways to counter heating that is often detrimental to electrophoretic devices. First, a significant source of heating at longer times is the exothermic reaction of water electrolysis products: protons and hydroxide ions. By removing these ions before they could react, this heating should be completely avoided. Other electrolysis products, particularly oxygen and hydrogen gas, were also removed in this step as previously noted. Second, the continual flow of room temperature buffer through the device carried away heat generated by Joule heating (resistive heating). The flow cell tolerated relatively high potentials and currents. With 1 mM buffer, the current was around 100 μA at an applied potential of 250 V (140 V/cm). When 10 mM NaCl was employed at an applied

potential of 250 V, the current was around 1 mAmp. Finally, a current around 10 mA was found with 100 mM NaCl in 1 mM Tris at the same applied potential.

TR-DHPE and Streptavidin Migration as a Function of pH. The mobility of Texas Red-DHPE and Alexa Fluor 488 labeled streptavidin with 4.0 dyes per protein molecule were observed at pH 3.3 and 9.3. These experiments were performed with 1 mM sodium citrate buffer and 1 mM Tris buffer, respectively. A field of 170 V/cm was applied for 10 min and the fluorescence images both before and after electrophoresis are shown along with corresponding line profiles. Initially, both the streptavidin (green curve) and Texas Red DHPE (red curves) were confined to approximately 400 μm wide strips. Under both sets of conditions, the Texas Red DHPE migrated to the right toward the anode (purple curves). This occurred because the net charge on the dye-labeled lipid molecule remained negative over this pH range. Throughout the pH range tested, the mobility of the Texas Red DHPE was 0.32±0.04 (μm/min)/(V/cm). One can also observe a small immobile fraction of the dye in both cases as a small peak left at the origin, possibly due to binding at surface damage associated with the scratch. The immobile fraction represented no more than 2% of the total Texas Red DHPE under all circumstances.

In contrast with Texas Red, the biotin-bound streptavidin behaved quite differently. The biomacromolecule moved to the left toward the cathode in the image at pH 3.3, while it moves to the right toward the anode at pH 9.3 (blue curves). In other words, the protein appeared to bear a net positive charge at pH 3.3 and a net negative

charge at pH 9.3. The mobility of the streptavidin varied between -0.6 (μm/min)/(V/cm) at pH 3.3 and 0.5 (μm/min)/(V/cm) at pH 9.3. In both cases, it should be noted that a somewhat more substantial fraction of the membrane-bound biomacromolecules were immobile compared with the lipid (~20%).

The electrophoresis experiments shown in Figure 3 were repeated as a function of pH between 3.3 and 9.3. The mobility values of the 4 dye-labeled streptavidin are plotted as a function of pH in Figure 4. The streptavidin mobility switched from a negative to positive value just below pH 5.0. It should be cautioned that this does not represent a true isoelectric point for the protein because the macromolecule was also subject to electroosmotic forces.[20] Indeed, the negatively charged substrate attracted cations (Na+), which flow toward the cathode. This electroosmotic flow also exerted a net force toward the cathode on the protein. The electroosmotic force on the streptavidin originates principally from the glass coverslip supporting the bilayer, as silanizing the glass viewing window in the device above the bilayer had no effect of the streptavidin mobility. However, the number of bound biotinylated lipids affected the pH of zero net streptavidin migration as each biotinylated lipid had a minus one charge. There can be either one or two bound biotin-DOPE molecules per streptavidin.[43,44] These bound lipid molecules will somewhat offset the effect of electroosmosis.

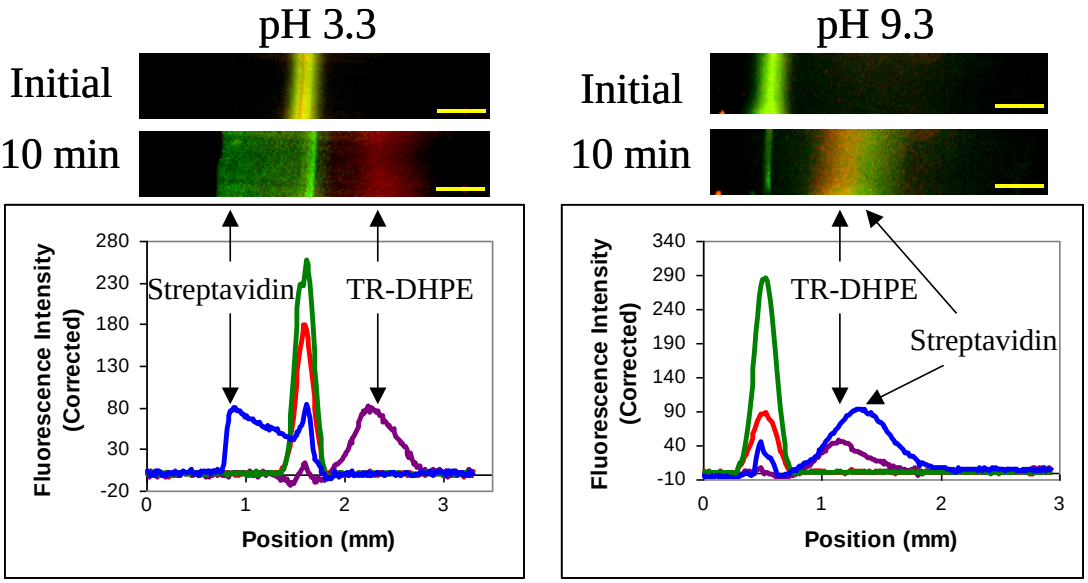

Figure 3. Typical electrophoresis results in 1 mM pH 3.3 sodium citrate (left) and 1 mM pH 9.3 Tris (right). False color fluorescence images (top) show the position of TR-DHPE (red) and streptavidin (green) initially (upper images) and after 10 minutes of applying a 170 V/cm field (lower images). Below these images are the corresponding fluorescence linescans with the initial intensities being depicted in green (streptavidin) and red (TR-DHPE) and the final intensities in blue (streptavidin) and purple (TR-DHPE).

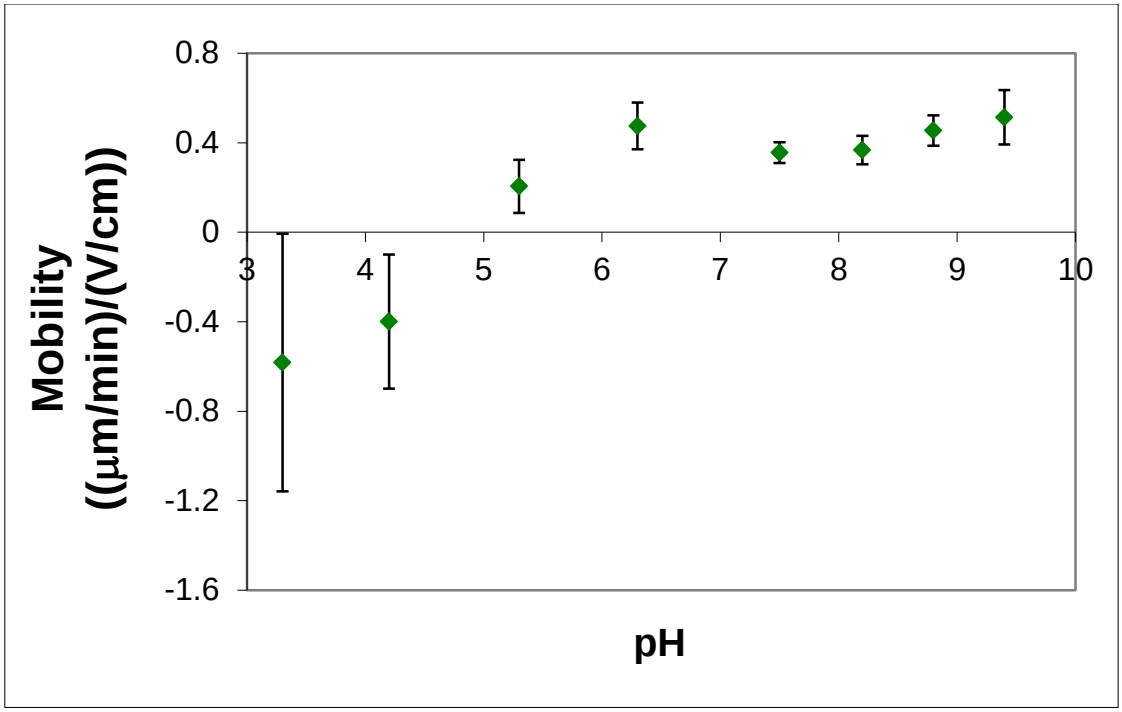

Figure 4. The mobility of streptavidin labeled with an average of 4.0 dyes/molecule as a function of pH at 170 V/cm. All runs were performed at 1 mM buffer concentration in a POPC SLB. Sodium citrate was used under acidic conditions (below pH 6), sodium phosphate at near-neutral conditions (6-7), and Tris under basic conditions (above pH 7). In this and all other figures, the error bars represent one standard deviation.

The electrophoretic mobility experiments with labeled streptavidin were repeated with 0.3 dye molecules per protein (Figure 5). Under these circumstances, the pH of zero net streptavidin migration became far more basic (~ pH 7). In fact, most of the observed protein molecules should have possessed a single label as the unlabeled molecules were not visible and very few molecules contain more than one label. The large shift in the isoelectric point was expected because the Alex Fluor 488 dyes were conjugated to free lysine residues on the protein surface via a succinimidyl ester. This is significant, because the free lysine bears a positive charge below pH ~10.3, while the dye is negatively charged. As such, four positive charges are converted to negative charges when the protein has four labels, but only one residue has its charge flipped when one dye is used. The pI for streptavidin has been reported to be between 5 and 6,[43,44] but this value clearly depends upon the degree of labeling, as more labeling should make the value more acidic. Such a result is consistent with literature data involving capillary electrophoresis measurements of green fluorescent protein as a function of labeling degree.[45]

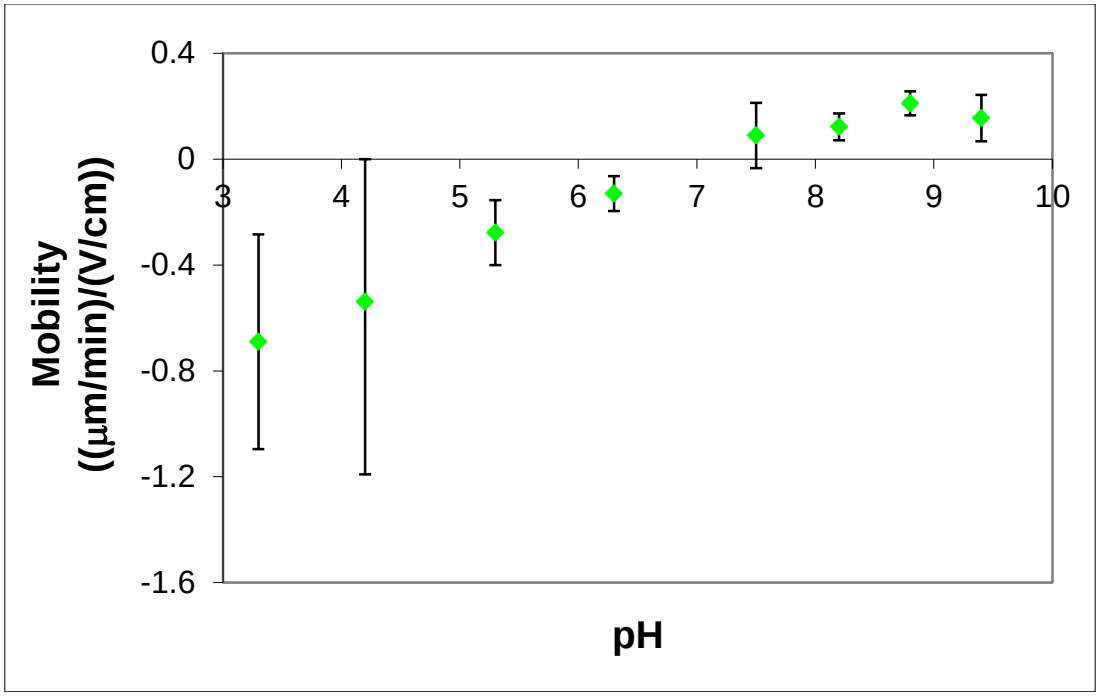

Figure 5. The mobility of streptavidin labeled with an average of 0.3 dyes/molecule as a function of pH at 170 V/cm. All runs were performed at 1 mM buffer concentration in a POPC SLB. Sodium citrate was used under acidic conditions (below pH 6), sodium phosphate at near-neutral conditions (6-7), and Tris under basic conditions (above pH 7).

Curiously, at pH 3 and 4, the electrophoretic behavior of streptavidin differed from its behavior under more basic conditions. Specifically, at higher pH values, the streptavidin migrated in a gradually broadening Gaussian peak as shown in Figure 3 at pH 9.3. At low pH, however, the streptavidin migrated as a front that slowed and stopped after 5 to 10 minutes. This led to the decidedly non-Gaussian shape seen at pH 3.3 in Figure 3. Both streptavidin with an average of 0.3 and 4.0 labels behaved identically in this respect. This implies that the effect was not only due to protein labeling. Rather, it seems likely that some structural change or partial unfolding may be occurring near pH 4 and below regardless of the labeling extent. This change may cause the streptavidin to aggregate and eventually stop electrophoretic motion completely. Aggregation of streptavidin under somewhat acidic conditions has been reported before, supporting this hypothesis.[46] Experiments at higher concentrations of biotin in the bilayer (2% as opposed to 1%) and thus streptavidin on the surface resulted in a larger immobile fraction of streptavidin, supporting the aggregation hypothesis. It should be noted that the electrophoretic mobility values reported in Figures 4 and 5 were taken within the first 5 minutes for the runs at pH 3 and 4. At all other pH values, the mobilities remained consistent over the course of 30 and even 60 minute runs.

Electrophoresis in PEG-Containing SLBs. In the next set of experiments, we wished to attenuate the electroosmotic contribution to the mobility of the fluorescently labeled membrane components. To do this, 0.5 mol% polyethyleneglycol linked phosphatidylethanolamine was added to the membrane. This concentration, near the

mushroom to brush transition, lifted the bilayer up away from the underlying negatively charged silica substrate by an amount similar to the Flory radius, in this case ca. 6 nm.[47,48] As such, it was removed from the diffuse double layer and the source of electromotic flow. Figure 6 compares the results of adding PEG to the separation SLB with simple POPC membranes. The data were taken with 0.3 dye/molecule streptavidin at 140 V/cm potentials in 1 mM buffers. As can be seen, the mobility of Texas Red DHPE was essentially unchanged by the addition of PEG. By contrast, the results for streptavidin are more pronounced. Under conditions far from the transition between the anodic and cathodic directions of travel, adding PEG slightly shifted the streptavidin mobility in the anodic direction (pH 5.2 & 9.3). Near the anodic to cathodic transition, adding PEG to the SLB completely reversed the direction of movement from cathodic to anodic (pH 6.3). Such a result is consistent with the notion that biotin-bound streptavidin bears a slightly negative charge under these conditions.[43,44] When the polymer cushion was absent, the protein moved toward the cathode because the electroosmostic force was dominant. In the presence of the PEG layer, this force was attenuated and the protein moved toward the anode based on its net charge.

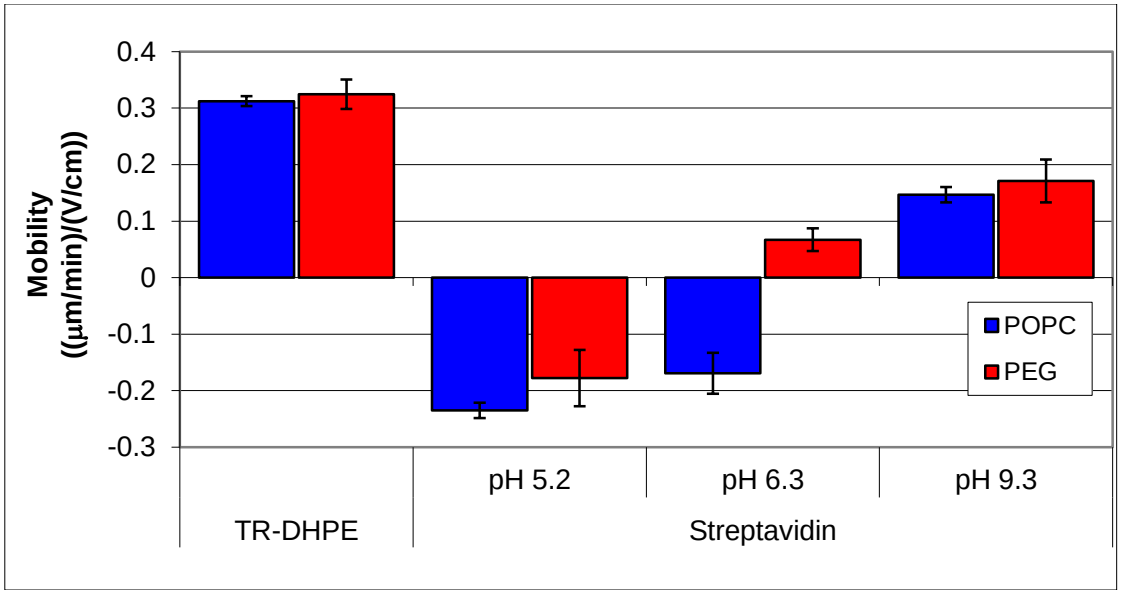

Figure 6. The mobility of TR-DHPE and streptavidin in POPC (blue) and in a POPC/PEG bilayer (red). The runs were performed in 1 mM sodium citrate (pH 5.2), sodium phosphate (pH 6.5), and Tris (pH 9.3) buffer with an applied potential of 140 V/cm.

Electrophoresis as a Function of Ionic Strength. A similar effect to that of adding PEG can be observed merely by modulating the ionic strength of the buffer. To do this, the electrophoretic mobility of streptavidin and Texas Red DHPE were observed with 0.5 mM citrate/0.5 mM Tris buffer containing 0 mM NaCl, 5 mM NaCl, and 10 mM NaCl. The mobility results at pH 7.9 with a field of 140 V/cm are given in Figure 7. As can be seen, the mobility of the Texas Red-labeled lipid was only slightly affected by the addition of salt. On the other hand, the streptavidin migration rate more than doubled. This occurred because increasing the ionic strength reduced the Debye length in the solution from 10 nm with the 0.5 mM buffer to 3-4 nm with the addition of 5 or 10 mM of NaCl.[49] Therefore, the charge on the glass support was more strongly screened at higher ionic strength. Also, there were probably more counterions between the bilayer and the support, which mitigates the field normal to the bilayer. As the streptavidin was confined to the upper leaflet of the bilayer, this reduced the electroosmotic force and allowed the negatively charged streptavidin to migrate faster toward the anode.

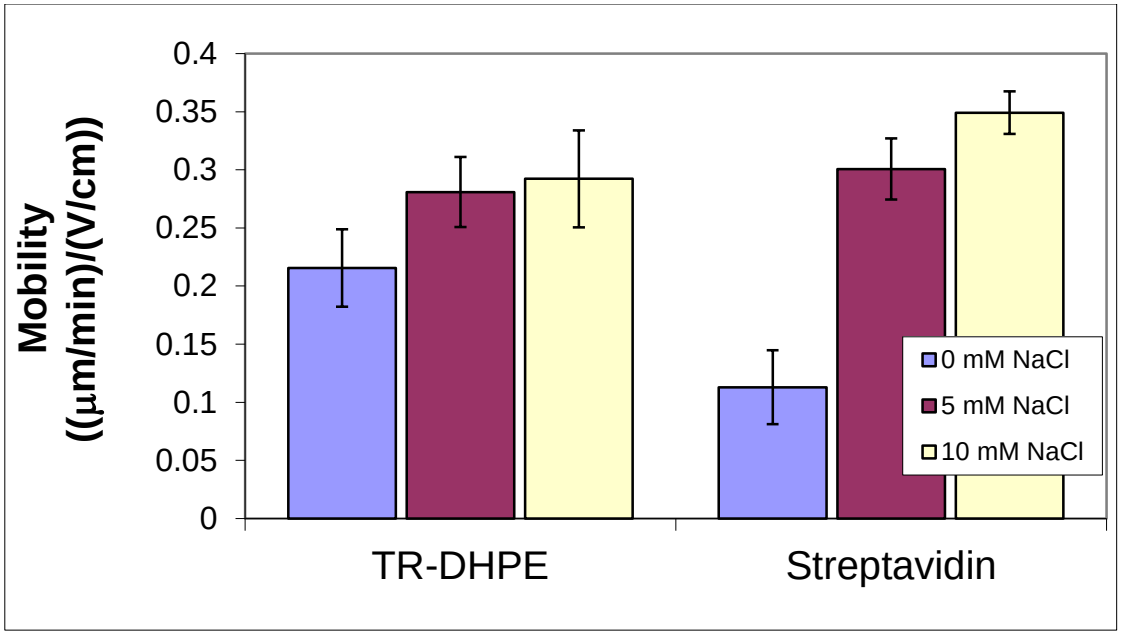

Figure 7. The mobility of TR-DHPE and streptavidin in POPC at different ionic strengths. All runs were performed in a pH 7.9, 1:1 sodium citrate/Tris buffer mixture for a total buffer strength of 0.5 mM. NaCl was added to the 0.5 mM buffer to make the 5 or 10 mM solutions. Electrophoresis was performed at 140 V/cm.

Conclusions

A flow cell has been constructed that allows the pH above a supported lipid bilayer to be continuously controlled during electrophoresis. Using this device, the response of membrane-bound streptavidin was investigated as a function of pH, the presence or absence of a PEG cushion support and the ionic strength. TR-DHPE served as a reference compound that was relatively insensitive to these variables. The electrophoretic migration of streptavidin was found to be highly pH dependent. At acidic pH values, the streptavidin migrated toward the cathode. At basic pH values, the protein migrated toward the anode. In both cases, electrophoretic and electroosmotic forces were present. The change in direction occurred as the charge on the streptavidin became sufficiently negative to counteract electroosmotic flow. Adding a PEG cushion to the bilayer or increasing the ionic strength also attenuated the electroosmotic force. Thus, both the electrophoretic and electroosmotic forces could be altered independently of one another. This suggests intriguing possibilities in the ability to precisely control the movement of membrane bound species in supported lipid bilayers.

CHAPTER IV

SUPPORTED LIPID BILAYER ELECTROPHORESIS COUPLED WITH MALDI-MS IMAGING: A NEW ANALYTICAL PLATFORM

Introduction

The phospholipid bilayer has many important roles in the physiological processes of cells. The versatility of the cell membrane is illustrated by the complexity of its lipid and protein composition. Understanding the interactions of the various components, their structure, and their physiological roles is of great importance to researchers trying to understand mechanisms of disease.

Supported lipid bilayer (SLB) systems have emerged as an important tool for creating models of the phospholipid bilayer in order to study the interactions and structure of various membrane components.[6-9] One avenue of study involves the development of electrophoresis systems that allow for the lateral separation of charged membrane components within the plane of the lipid bilayer.[18,21] Recent studies have improved the ability to separate multiple species bearing the same charge by introducing a heterogeneous SLB system.[22] In these systems analyte containing SLBs were patterned into a background SLB whose composition was tuned to optimize separation conditions. Developments in cushioning architectures have increased the mobile fraction of transmembrane proteins embedded in SLBs.[13,15,17] Additionally, our group recently demonstrated the importance of maintaining strict control over the buffering environment of SLBs during electrophoresis, particularly for proteins, and developed the

required technology.[23,50] Each of these accomplishments is critical towards developing a method capable of separating and studying membrane proteins within their native environment: the lipid bilayer.

Traditionally, separations in lipid bilayers have been monitored by fluorescence microscopy.[18,21-23,50] While such light-based optical imaging is an effective analytical tool for measuring the mobility of membrane bound species in the plane of the bilayer, the use of extrinsic molecular tags (*e.g.*, fluorophores) imposes limitations and possible complications to the experiments.[24] The conjugation of a fluorophore to an analyte can affect the analyte's mobility in the bilayer by altering both its size and net charge.[23,45,50] Additionally, conjugation may occur at a site that can inhibit interactions between analytes. Lastly, there are only a finite number of fluorescent tags that can be employed within a single system without spectral overlap, which ultimately leads to a limitation in the number of different species that can be detected.

A technique that has promise for spatially resolving and characterizing membrane species is imaging mass spectrometry (MS).[51-53] Imaging MS is inherently a label-free method, due to the use of an analyte's mass to charge ratio (*m/z*) for detection. While secondary ion MS (SIMS) is capable of imaging many components of SLBs,[54] it suffers from a narrow mass range, typically <1 kDa, and a high degree of analyte fragmentation.[55] Matrix assisted laser desorption ionization (MALDI) MS has been utilized to image complex biological samples (*e.g.*, tissue specimens). MALDI-MS has the ability to produce large intact singly charged molecular ions; these ions generate deconvoluted spectra, which allows for simple analyte identification.[53] While imaging

MALDI-MS does not have the spatial resolution of SIMS, it is adequate for this application. Additionally, the required imaging area for these separation studies (~3 mm x 1 cm) exceeds the practical sampling area for SIMS, but can be facilely accomplished by MALDI-MS imaging. As such, MALDI-MS imaging could potentially map the location of hundreds of membrane components in an SLB.

Herein, we report the separation of the most complex mixture of membrane components by SLB electrophoresis to date. Additionally, this is the first separation of two naturally occurring cell surface receptors using SLB electrophoresis. The lipid receptors, monosialoganglioside GM1 and disialoganglioside GD1b, play several important physiological roles and have been implicated in disease pathways via cell-pathogen docking.[56-58] In these experiments, *ortho*- and *para*- Texas Red DHPE, two fluorophore-labeled lipids, were used to monitor the real-time progression of electrophoresis. MALDI-MS imaging was utilized to create an ion map of the SLB that revealed the location of each membrane species after electrophoretic separation.

Experimental

Materials. Cholesterol (Chol), 1-palmitoyl-2-oleyl-*sn*-glycero-3-phosphocholine (POPC), 1,2-dieicosenoyl-*sn*-glycero-3-phosphocholine (DEPC), and1,2-dilauroyl-*sn*-Glycero-3-phosphocholine (DLPC) were purchased from Avanti Polar Lipids (Alabaster, AL). Monosialoganglioside GM1 and disialoganglioside GD1b were both purchased from Sigma (St. Louis, MO). The fluorescently labeled lipid, Texas Red 1,2-dihexadecanoyl-sn-glycero-3-phosphoethanolamine (TR-DHPE) was purchased from

Invitrogen (Carlsbad, CA) and contained a mixture of the ortho- and para- isomers. Glass slides and coverslips were purchased from Corning (Corning, NY). Polydimethylsiloxane (PDMS) was produced using a Dow Corning Sylgard Silicone Elastomer-184 Kit (Midland, MI).

Preparation of Glass Substrates. Corning coverslips (No. 1 ½, 24x40mm) were rinsed, boiled in 1:7 diluted 7X® detergent in water (MP Biomedicals, Solon, OH), thoroughly rinsed with 18 MΩ water, blown dry with nitrogen and then annealed at 530°C for 5 hrs. These substrates were stored in a clean manufacturer's container for up to two weeks before use.

Preparation of Vesicles. Small unilamellar vesicles (SUVs) were prepared using the freeze-thaw/extrusion method.[38,39] Briefly, lipids dissolved in chloroform (or methanol:chloroform, 1:2, in the case of the gangliosides) were mixed in the desired mole ratios and the organic solvents were evaporated under a stream of nitrogen followed by complete solvent removal under vacuum overnight. The two vesicle compositions used in these experiments were (i) 10% GD1b, 3% GM1, 2% TR-DHPE, 85% POPC and (ii) 25% Chol, 37.5% DLPC, 37.5% DEPC. The desiccated lipid mixtures were rehydrated in PBS (10 mM sodium phosphate buffer and 150 mM NaCl, pH 7.5) and subjected to 10 freeze/thaw cycles using liquid nitrogen and warm water. The vesicle solutions were extruded 10 times through a polycarbonate filter containing 100 nm pores (Whatman, Florham Park, NJ), diluted to 1 mg/ml, and stored at 4˚C until

further use. Vesicles were found to have a sharp distribution around 100 nm using a 90Plus Particle Size Analyzer (Brookhaven Instrument Corp., Holtsville, NY).

Preparation of PDMS Wells and Stamps. Polydimethylsiloxane (PDMS) was used to create wells for containing the SLBs. Sheets of uniform thickness (150±15 μm) were created by polymerizing the PDMS between two annealed/silanized glass slides. These sheets were cut to the dimensions of the glass coverslips and a channel of ~2.2 cm by 4 mm was cut into their centers. These wells were cleaned and applied to the glass substrate and all bubbles between the PDMS and glass were removed via mechanical pressure. PDMS stamps were created in a similar manner, but the polymer films were ~2 mm thick. The stamps were cut to have a foot print of ~3 mm by 600 μm, then rinsed with nanopure water and ethanol, blown dry with nitrogen, oxygen plasma cleaned for 1 min bottom-side-up, followed by placement in the desired location of the PDMS well.

Preparation of Heterogeneous Supported Lipid Bilayers. SLBs were created using the vesicle fusion method.[6,21,40] Once the PDMS well and stamp were positioned on the coverslip, 50 μL of the primary vesicle solution was used to create the separation SLB. After 5 minutes, the well was thoroughly rinsed and stamp removed. Next, 20 μL of the secondary vesicle solution was added along with 20 μL of 4M NaCl. NaCl screens the negative charge repulsion between the analytes and substrate, facilitating the vesicle fusion process.[59] The vesicle solutions were allowed to incubate for 5 minutes before thoroughly rinsing with purified water. This process created a discrete secondary SLB

(the origin) inside a larger primary SLB (separation region), as illustrated in Figure 8A-C.

Supported Lipid Bilayer Electrophoresis. The heterogeneous SLB was coupled to an electrophoretic flow cell device, described previously.[23] Briefly, the device allows electrophoresis to occur under constant buffering conditions while removing the products of electrolysis and mitigating joule heating. These experiments were performed under a constant flow of 100 μM phosphate buffer (no NaCl, pH 7.8, ~1.5 mL/min flow rate) for 1 hr at 600 V (average current ~35 μA). No measurable pH variations were observed under these conditions. Electrophoretic separation of the TR-DHPE *ortho*- and *para*- isomers was monitored in real-time using an epifluorescence microscope.

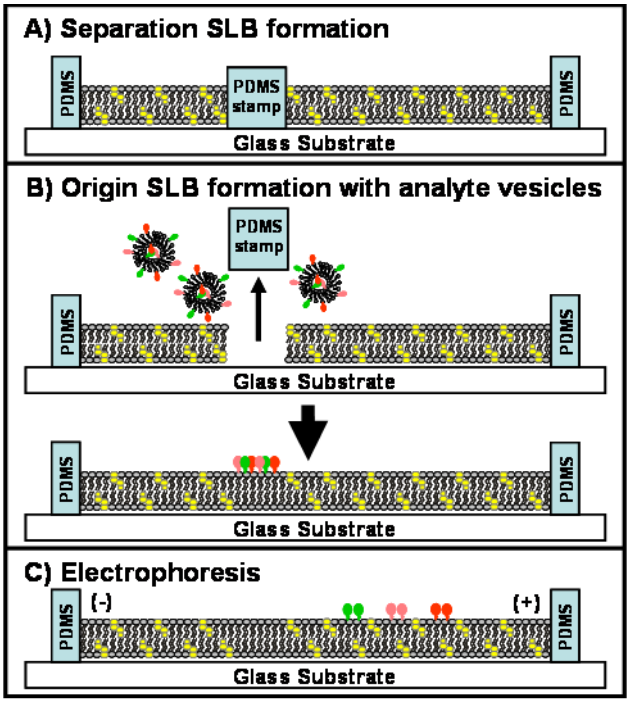

Figure 8. Schematic representation of the stamp method used for heterogeneous SLB preparation. A) The separation SLB was formed in the PDMS well with the PDMS stamp in place. B) After rinsing, the PDMS stamp was removed and analyte vesicle solution added, followed by another rinsing step. C) During electrophoresis charged analytes (lipids, etc.) migrate from the origin and into the separation region. Yellow molecules in the bilayer represent cholesterol.

Supported Lipid Bilayer Freeze-Drying. After electrophoresis the flow cell was deconstructed under water. The coverslip with its intact PDMS well was carefully brought out of the bath under a gentle water stream from a squirt bottle. Excess water was removed from the coverslip via pipette, until ~30 μL remained. The hydrated SLB was quickly plunged into liquid N_2 cooled liquid ethane. The sample was placed in a sample holder that used liquid N_2 to keep the sample stage cool without allowing the sample to touch the liquid nitrogen. This was placed in a pre-chilled desiccator contained in a box freezer. Once the evaporation of the liquid nitrogen inside the container had subsided (pressure equilibrated) the desiccator was attached to a vacuum line and remained under vacuum for ~8 hrs, or until all the ice in the well had sublimed away. The desiccator was removed from the freezer and allowed to reach room temperature while still under vacuum. The sample's integrity was checked using fluorescence microscopy, prior to MS analysis. Slight fissures in the bilayer (cracks) and small amounts of delaminated vesicles (bright dots) were detected, but otherwise the bilayers were observed to be macroscopically intact.

Matrix Application. The coverslip bearing the freeze-dried SLB was mounted on a glass slide and sprayed with MALDI matrix. Optimized matrix and solution conditions were composed of 10 mg/mL alpha-cyano-4-hydroxycinnamic acid, 30 mg/mL 2,5-dihydroxybenzoic acid, and 20 mM diammonium citratate in 10 mL of 2:1:0.03 acetone:methanol:water. Matrix solution was uniformly sprayed onto the freeze-dried sample using an airbrush gun powered by 30 psi N_2 gas from a cylinder. The airbrush

was held ~6 inches from the sample during application. The matrix was applied by slowly passing the brush back and forth over the sample, allowing the solvent to dry between passes.

Mounting the Sample to a MALDI Plate. The coverslip was mounted on a clean MALDI plate using two strips of two-sided copper tape. After removal of the PDMS well, a clean nickel grid (70 lines per inch) was placed over the sample and secured in place using single-sided copper tape. Care was taken to ensure the grid was completely flat across the sample and the copper tape was in full contact with the MALDI plate. The grid was used to circumvent charge buildup from the glass surface upon analyte ionization in the mass spectrometer.

Imaging Mass Spectrometry. Bilayer samples were investigated on a 4700 Proteomics Analyzer MALDI TOF/TOF (Applied Biosystems, Foster City, CA) mass spectrometer under optimized conditions in reflection mode. The mass spectra were externally calibrated using standards spotted on mounted glass substrate. The laser spot size was observed to be an ellipse with dimensions of 60 x 100 μm. Therefore, the laser was rastered over the sample with a step size equal to those dimensions using 4700 imaging software (Novartis and Applied Biosystems). Individual mass spectra represent the average of 250 laser shots and BioMap software (Novartis, Basel, Switzerland) was used to generate ion-specific maps of the sample. Mass assignments were validated by comparison to spectra taken from pure reagents.

Results and Discussion

Heterogeneous SLB Preparation. The invention of heterogeneous SLBs for use in bilayer electrophoresis was an important step towards being able to perform more complex separations as it allowed for the construction of distinct separation and origin regions. This independence in composition between the two regions allows them to be tuned to optimize separation of the analytes.[22] Heterogenous SLBs were previously constructed using a 'scratch and backfill' method, which generated ~100 μm wide analyte containing origin regions. Examination of a 'scratch and backfill' system at higher magnification reveals that the origin region is actually a succession of narrow scratches, due to the micron scale roughness of the utensil used. Thus, the actual composition of the origin region is a mixture of the two regions. In this work, PDMS stamps were utilized to create a heterogeneous SLB system, as outlined in Figure 8. While using a stamp to pattern a heterogeneous SLB produces a broader (~600 μm) origin line, it allows for a greater amount of analyte containing SLB to be deposited and provides a sharper interface between the two SLB regions in the system.

Heterogeneous SLB Electrophoresis. The focus of this work is to develop a technique to observe the location of membrane species post-electrophoresis without the use of extrinsic tags; however, a small amount of fluorescent reporter is useful in discerning the quality of both the SLB pattern and electrophoresis (Figure 9A-D). While the dogma of separations chemistry argues that one should use as narrow of an origin as possible for optimal separation, compromises are required due to the limitation of MALDI-MS

imaging resolution dictated by the laser spot size. However, just as gel electrophoresis has utilized stacking layers to concentrate the contents of the well prior to separation, the viscosity of the separation medium can be exploited to mitigate the drawbacks of a broad origin. The use of cholesterol solely in the separation region causes the analytes to build up at the SLB interface before entering the separation region, as seen in Figure 2A-C. This phenomenon is due to the difference in bilayer viscosity between the two SLBs, which is a function of their cholesterol content (0% in origin vs. 25% in separation SLB). As a result, the 600 μm origin line narrows to nearly 200 μm before appreciable separation begins. While the high cholesterol content of the separation SLB lowers diffusional broadening, this phenomenon can never be fully negated. In this experiment the modest broadening observed after electrophoresis (Figure 9D) indicates the power of heterogeneous SLBs.

A cartoon representation of the heterogeneous SLB system before and after electrophoresis is shown in Figure 9E. This depiction of the SLB system shows the other three analytes; all of which are naturally occurring species and undetectable with fluorescence microscopy. In order to visualize the location of SLB components lacking extrinsic tags, MALDI-MS imaging was utilized.

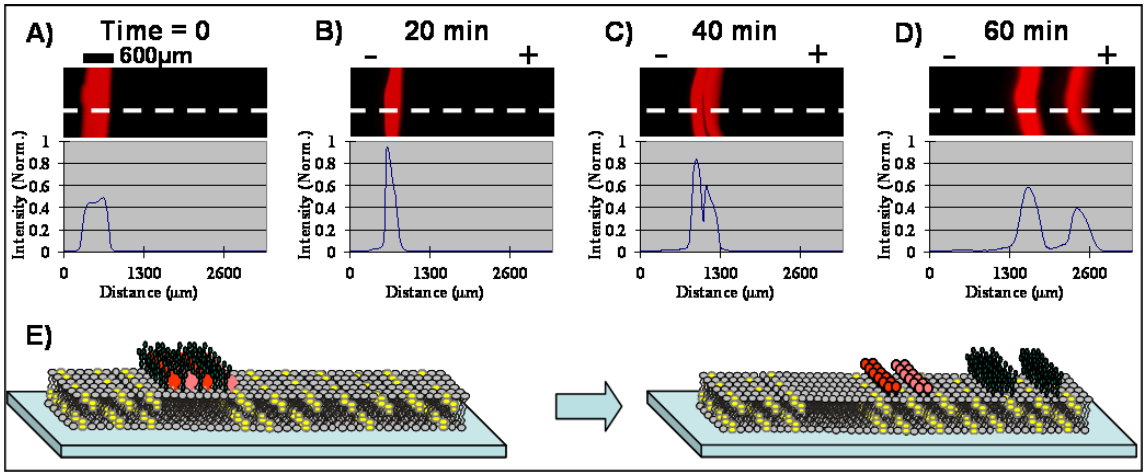

Figure 9. Time lapsed micrographs of an electrophoretic separation. A-D) Fluorescent images (via TxRed-DHPE) and lines scans show the progression of analyte separation during electrophoresis. Graphs illustrate the analyte band narrows and increases in intensity (concentrates) at the perimeter of the origin SLB before proceeding into the separation region. E) A cartoon illustrating the separation of the five analytes, including the species that are not fluorescently labeled.

SLB Preparation for MS Imaging. To interrogate the SLB with MALDI-MS the sample had to be removed from its hydrated environment and made vacuum compatible without causing macroscopic surface rearrangement. A schematic for this process can be seen in Figure 10A. The fluorescent images (Figure 10B-E) clearly illustrate that the SLB does not undergo any major surface reorganization during the process. It should be noted that freeze-drying, airbrush matrix deposition, and MALDI plate mounting are all somewhat delicate techniques that require practice to prevent reorganization of the surface. MALDI-MS imaging researchers have suggested various methods of mounting tissue samples to MALDI plates and procedures to apply matrix.[60] In this report, the sample is a dried lipid film on a glass (insulating) substrate. To overcome the ion suppression effects, conductive copper tape and a Ni grid were used to dissipate the accumulation of charge at the analyte ionization surface. Figure 10F shows the laser ablation spots and indicates the area sampled via MS imaging.

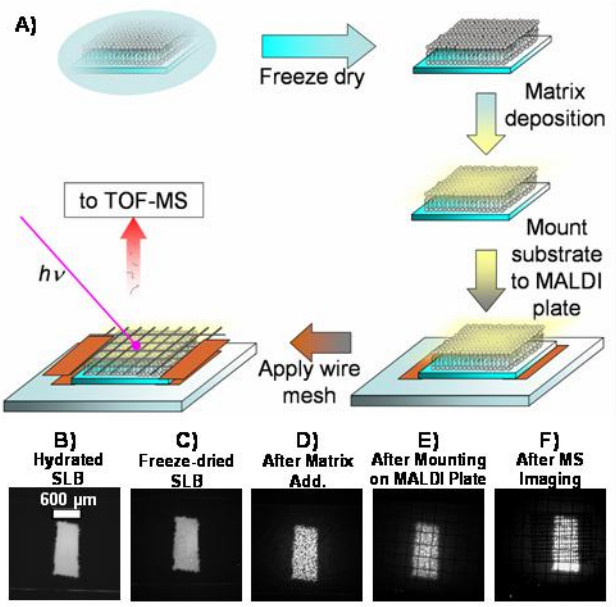

Figure 10. SLB preparation for MALDI-MS imaging. A) Schematic diagram of the sample preparation process used to prepare the SLB for MS analysis. The hydrated lipid bilayer is freeze-dried and prepared for MS analysis by matrix application and mounted to a MALDI plate with a Ni grid using Cu tape. B-F) Fluorescence images (via TxRed-DHPE) showing each step of the process and demonstrating that there are no major surface rearrangements during the sample preparation process.

MALDI-MS Imaging of the SLB. Imaging MALDI-MS was used to map the position of each component in the SLB before and after electrophoresis. Figure 11 shows multiple ion-specific images of the heterogeneous SLB before electrophoresis. The fluorescence image of the SLB (Figure 11A) indicates the regions that were analyzed using imaging MS. The black ovals in the fluorescence image are the ablation spots from which the mass spectra were obtained. The top portion of the sample was imaged in negative ion mode in order to locate the positions of GM1 and GD1b. The bottom half of the sample was imaged in positive ion mode in order to locate the positions of POPC and DLPC. It should be noted that one could easily alter the raster pattern to an alternating pattern of positive mode rows and negative mode rows to compensate for abnormalities and non-uniformities in the bands imaged. In summary, all the components of the origin SLB (Figure 11B-D) were clearly segregated from the separation SLB (Figure 11E) prior to electrophoresis.

The mass spectra in Figure 11F-H, represent those used to produce the ion specific images in Figure 11B-E. In the negative mode spectra taken from the origin SLB (Figure 11E), the GM1 (*m/z* 1545 and 1573, corresponding to [GM1(18:0/d18:1) - H]$^-$ and [GM1(20:0/d18:1) - H]$^-$, respectively) and the GD1b (*m/z* 1792-1886, fully described in supplemental information) are clearly present. GM1 (*m/z* 1454) and GD1b (*m/z* 1836) were the specific signals used to generate the images in Figure 11B and 11C, respectively. The positive mode spectra taken from the origin SLB (Figure 11F) shows a predominate signal from POPC (*m/z* 761 and 783, corresponding to [POPC + H]$^+$ and [POPC + Na]$^+$, respectively). POPC (*m/z* 761) was used to generate the image in Figure 11D. The positive mode spectra taken from the separation SLB (Figure 11H) shows a predominate signal from DLPC (*m/z* 622 and 644, corresponding to [DLPC + H]$^+$ and [DLPC + Na]$^+$, respectively). DLPC (*m/z* 622) was used to generate the image in Figure 11E.

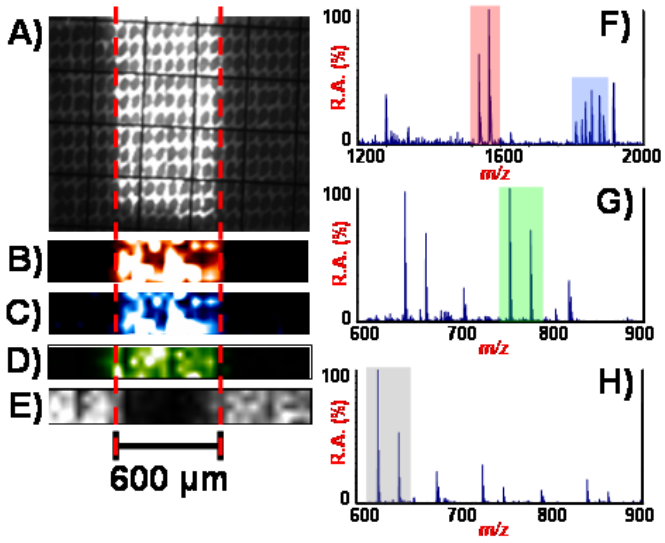

Figure 11. MALDI-MS imaging of a heterogeneous SLB prior to electrophoresis. A) Fluorescence image of a heterogeneous SLB after imaging MS. Black spots are the ablation spots from the MALDI-MS laser. Ion-specific images of the SLB components: B) GM1, C) GD1b, D) POPC, and E) DLPC. Ion-specific images shown in B and C were acquired in negative ion mode, whereas ion-specific images in D and E were acquired in positive ion mode. F) Negative ion mode mass spectra of the orig0in SLB showed four analytes; *ortho*- and *para*- TxRed-DHPE (*m/z* 1279), GM1 (*m/z* 1545 and 1573), GD1b (*m/z* 1792-1886). G) Positive ion mode mass spectra of the origin SLB show peaks indicative of POPC (*m/z* 761 and 783). H) Positive ion mode mass spectra of the separation SLB show peaks for DLPC (*m/z* 622 and 644).

Figure 12A-D shows ion-specific images of an SLB sample using the same components and construction as outlined in Figure 11, but after electrophoresis. Figure 12E is a composite of the individual ion-specific images after electrophoresis. All five components of the origin SLB (POPC, *para*-TxRed-DHPE, *ortho*-TxRed-DHPE, GM1, and GD1b) were separated from each other. Representative mass spectra in Figure 12G-I show the presence of analyte-specific ions and indicate the purity of each separated analyte band. Ions present at *m/z* 1545 and 1573 in Figure 12I are due to a loss of sialic acid (291 Da) from GD1b; these results have been previously observed.[61]

The origin is marked by POPC (Figure 12D), which exhibits no electrophoretic motion during the separation due to its net neutral charge under the current buffering conditions. The TxRed-DHPE isomers and gangliosides migrated out of the origin towards the anode due to their negative charge states under the current buffering conditions. The singly charged TxRed-DHPE isomers migrate significantly slower than the singly charged GM1, despite the similarity in acyl chains (supporting info). This result was explained by molecular simulations, which describes that the TxRed-DHPE head group spends most of its time located in the hydrophobic (highly viscous) region of the bilayer.[62] This orientation produces a high drag force resulting in a slower electrophoretic velocity.

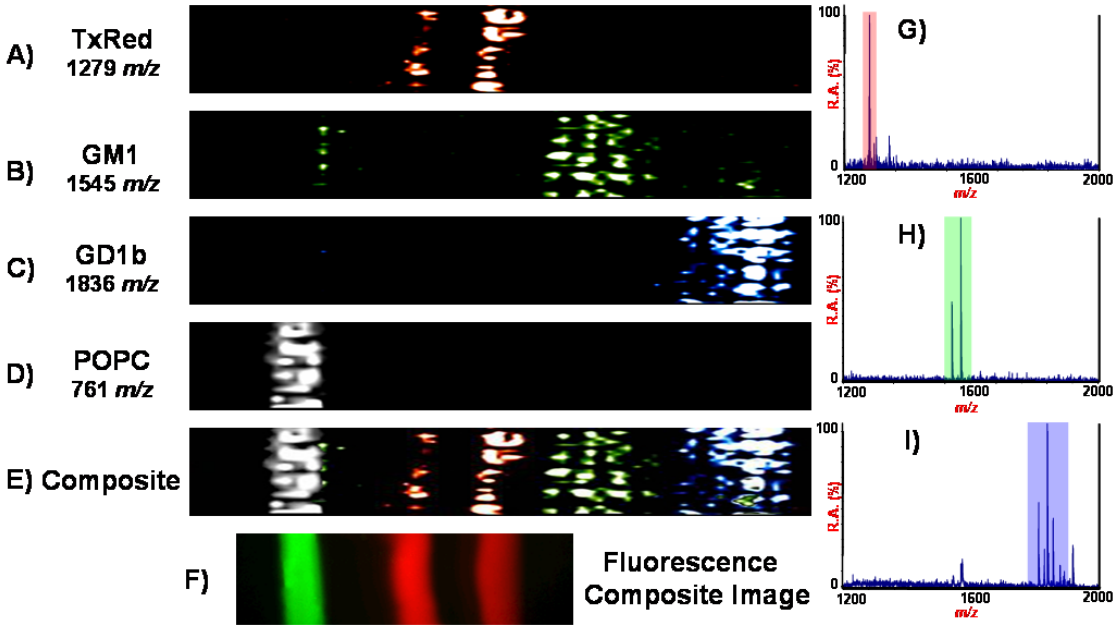

Figure 12. MALDI-MS imaging of a heterogeneous SLB post electrophoresis. A-D) Ion-specific images of the SLB components: A) TxRed-DHPE, B) GM1, C) GD1b, D) POPC. E) A composite image overlaying the ion-specific images from A-D, illustrating the separation of the five analytes. F) A composite image of two fluorescence images; the green is the origin prior to electrophoresis and the red bands are the two TxRed-DHPE isomers after SLB electrophoresis. Images in E and F show agreeable spatial distribution of the components. G-I) Representative mass spectra taken from regions indicated in A, B, and C; demonstrating analytes were baseline separated from one another. G) *ortho*- and *para*- TxRed-DHPE (*m/z* 1279). H) GM1 (*m/z* 1545 and 1573). I) GD1b (*m/z* 1792-1886).

In contrast, the gangliosides' (GM1 and GD1b) hydrophilic head groups have minimal interaction with the bilayer's hydrophobic core.[63] The gangliosides separate from each other because of differences in charge (a function of the number of sialic acid groups in each); GM1 (-1) migrates more slowly than GD1b (-2). A composite of two fluorescence images (Figure 12F), taken before (green) and after (red) electrophoresis, illustrates the agreement in spatial distribution between the fluorescence data and the MS imaging data.

This work brought together developments in SLB construction, electrophoresis, and MALDI-MS imaging technologies to develop a new analytical tool for biochemistry and biophysics. The ability to produce high quality heterogeneous SLBs, carry out electrophoresis under tightly controlled buffering conditions, and utilize label-free imaging is valuable for both separations and the ability to study intra-membrane interactions. Strategic placement of membrane components in the origin followed by monitoring their migration pattern will reveal valuable information about their relationship. For example, if two membrane components such as a membrane protein and a specific lipid are believed to form a complex in the plane of the membrane, these combined techniques could be used to probe the existence of a complex by monitoring for co-migration vs. independent migration using a label-free approach. Using this combination of techniques, we now have the opportunity to probe the relationship between a variety of unlabeled membrane components (e.g., lipid-lipid, protein-protein, protein-lipid, lipid-small molecule, etc.) and provide currently inaccessible information about complex formation under native conditions.

The combination of MALDI-MS imaging and SLB electrophoresis offers a unique platform for the separation and study of membrane components and their complexes. While MS detection allows extrinsic labels to be avoided, SLB electrophoresis allows membrane component separation to take place while avoiding the detergent solubilization conditions often required for traditional separation techniques. Analyte ion suppression effects in complex biological mixtures are the driving force behind utilizing separation techniques to pre-fractionate the analytes prior to MS analysis.[64] SLB electrophoresis now shows promise at being able to fill the role of pre-fractionating membrane components prior to MS analysis. This technology presented is currently being adapted to study *E. coli* inverted inner membrane vesicle derived SLBs, which are discussed in more detail in the next chapter.

Conclusion

In conclusion, this work clearly shows the capability to couple SLB separations and MALDI-MS imaging technologies in order to develop a new analytical platform for the separation and detection of membrane components from vesicles containing a mixture of analytes. This work is the first to separate five membrane components using SLB electrophoresis and the first to use MALDI-MS imaging to show the spatial distribution of components within a heterogeneous SLB. Additionally, this is the first report of the separation of two naturally occurring cell surface receptors using SLB electrophoresis. While this work only shows the separation and subsequent imaging of lipid species, experiments are ongoing to image SLB separations of peripheral and

integral membrane proteins, with the eventual goal of separating and imaging components from native membranes.

CHAPTER V

PATTERNING AND SEPARATING NATIVE MEMBRANES FROM *E. COLI*

Introduction

In order to better understand the complex nature of the cell membrane, researchers have extensively utilized supported lipid bilayers (SLBs) as models.[10] These systems have been used to study the biophysics within the plane of the membrane, its structure, and investigate the interactions of membrane bound receptors with soluble ligands.[65-71] This technology has even crossed over from being used for understanding fundamental science to application-driven biosensor and separation technologies.[72,73] The systems used, however, have always been relatively simplistic in terms of component composition compared to the native cell surface.[10] While much has been learned from these studies, the limitation of functional protein incorporation into these systems leaves them inadequate as models for understanding the majority of the native cell membrane's physiological processes.

To remedy this short-coming, the methodology to produce membrane protein containing supported lipid bilayers with high lateral mobility has been intensely pursued over the last few decades.[17] The primary limitation is the structure of the supported lipid bilayer, in which the complex mixture of van der Waals, hydrophobic, electrostatic, and steric interactions produce only a ~1 nm thick hydration layer between the bilayer and its support.[59,74,75] This distance is inadequate for accommodating protein species that protrude from the lower leaflet, becoming immobilized and possibly denatured on the underlying substrate. In order to increase the spacing between the bilayer and its solid support, researchers have tried a number of cushioning strategies from adsorbed cellulose films to the

use of tethers and spacers.[17] However, only a few of the many cushion designs have proven useful for studying transmembrane protein mobility.[13,14,25,26] Of these methods, the use of polymer-modified lipids as cushions seems to show the most promise.

The first use of poly(ethylene glycol) (PEG) modified lipids for the production of mobile bilayers by Tamm and co-workers showed a significant increase in mobile fraction of annexin V and cytochrome b5 compared to simple supported bilayers on quartz.[25] While increases in the mobile fraction of membrane proteins were accomplished in this study, the majority of the mobile protein populations had extremely low diffusion coefficients, presumably due to the increased drag force created by using tethers as cushions. Stemming from this work, our group investigated the use of PEG-modified lipids that were not connected to the substrate.[15] Additionally, a passivation layer of bovine serum albumin (BSA) was used. This "double cushion" architecture produced drastically increased mobile fraction percentages and diffusion coefficients for annexin V containing bilayers. Recently, the use of PEG tethers was revisited with dramatic increases in both percent mobile fraction and diffusion coefficients of both lipid and a reconstituted chimeric transmembrane protein.[16]

Another area of research within the realm of supported bilayer investigations has focused on developing the manipulation of membrane components with external electric fields. Charged lipids, lipid anchored proteins, and adsorbed DNA has been manipulated in this manner.[18,20,76,77] Indeed, even separations of complex lipid mixtures[22] and lipid anchored protein mixtures[50] have been reported. However, there has been only one report to date about the electrophoretic manipulation of a transmembrane protein within a SLB.[78] Recently, Evans and co-workers demonstrated the ability to concentrate CymA, a protein with a α-

helical membrane spanning domain. This protein lacks the large protruding extra-membrane domains, which are the primary obstacle to transmembrane protein mobility within a SLB.

The authors of these membrane component manipulation studies always tout that the reported methodologies will be used to 'eventually' separate membrane components from native membranes for proteomics purposes. However, the ability to create highly mobile SLBs from native membranes has yet to be accomplished. The reports in which native membranes were spread onto cushioned solid supports show no diffusion of the membrane species within.[79,80] Recent work by Hook and co-workers demonstrated that a SLB could be hydrodynamically driven into a fibroblast vesicle to create a continuous SLB incorporating the fibroblasts membrane components; however, only lipid mobility was reported.[81]

All the puzzle pieces have been revealed. In order to produce an analytical method that will be able to separate lipids and proteins from a native membrane for membrane proteomics, one must simply put the pieces of the puzzle together. Utilizing the latest SLB electrophoresis techniques for complex mixture separations, a cushioning architecture that will prevent membrane proteins from denaturing on the solid support, and methods to incorporate native membrane species into continuous SLBs the breakthrough which hath been prophesized has finally arrived.

Herein, we report on the incorporation of native membranes from *E. coli* into a double cushioned heterogeneous SLB architecture that allows for the separation of both lipids and membrane proteins. Inverted inner membrane vesicles (IMVs) of *E. coli* were mixed with PEG-modified lipids and fused to a BSA passivated surface to produce a highly mobile SLB. This vesicle fusion approach was then coupled with the micro-patterning technique used to produce heterogeneous SLBs for electrophoresis experiments. This report

contains the unprecedented methodology required to separate lipids and membrane components directly from native membranes without the use of organic solvents or detergents.

Experimental

Materials. Cholesterol (Chol), 1-palmitoyl-2-oleyl-sn-glycero-3-phosphocholine (POPC), N-palmitoyl-sphingosine-l-{succinyl[methoxy(polyethylene glycol)5000] (PEG5Kce) were purchased from Avanti Polar Lipids (Alabaster, AL). Texas Red 1,2-dihexadecanoyl-sn-glycero-3-phosphoethanolamine (TR-DHPE), Alexa Fluor 594 carboxylic acid succinimidyl ester were purchased from Invitrogen (Carlsbad, CA) and each product contained a mixture of isomers. Also, Alexa Fluor 488 goat anti-rabbit IgG (H+L) and YO-PRO-1 Iodide (491/509) were purchased from Invitrogen (Carlsbad, CA). Bovine serum albumin (BSA) was purchased from Pierce (Rockford, IL). Glass slides and coverslips were purchased from Corning (Corning, NY). Polydimethylsiloxane (PDMS) was produced using a Dow Corning Sylgard Silicone Elastomer-184 Kit (Midland, MI).

Preparation of Glass Substrates. Fisherbrand coverslips (No. 1 ½, 24x40 mm) were rinsed, boiled in 1:7 diluted 7X detergent in water (MP Biomedicals, Solon, OH), thoroughly rinsed with 18 MΩ water, blown dry with nitrogen and then annealed at 530°C for 5 hrs. These substrates were stored in a clean manufacturer's container for up to two weeks before use.

Preparation of Vesicles. Small unilamellar vesicles (SUVs) were prepared using the freeze-thaw/extrusion method.[38,39] Briefly, lipids dissolved in chloroform were mixed in the desired

mole ratios and the organic solvents were evaporated under a stream of nitrogen followed by complete solvent removal under vacuum overnight. The three vesicle compositions used in these experiments were (i) 0.5% PEG5Kce, 99.5% POPC, (ii) 0.1% TR-DHPE, 0.5% PEG5Kce, 99.4% POPC and (iii) 20% Chol, 0.5% PEG5Kce, 79.5% POPC. The desiccated lipid mixtures were rehydrated in TBS (10 mM Tris buffer and 100 mM NaCl, pH 7.5) and subjected to 10 freeze/thaw cycles using liquid nitrogen and warm water. The vesicle solutions were extruded 10 times through a polycarbonate filter containing 100 nm pores (Whatman, Florham Park, NJ), diluted to 1 mg/ml, and stored at 4˚C until further use. Vesicles were found to have a sharp distribution around 120 nm using a 90Plus Particle Size Analyzer (Brookhaven Instrument Corp., Holtsville, NY).

Preparation of Inner Membrane Vesicles. Inverted inner membrane vesicles (IMVs) were obtained from Siegfried Musser's lab. Two types of *E. coli* MC4100 IMVs were used in this report. One was produced from a knock-out strain (ΔTatABCDE), which had the Twin-Arginine Translocase proteins TatA, TatB, TatC, TatD, and TatE deleted. The other was produced from a strain with TatA, TatB, and TatC overexpressed. The IMVs were further purified by methods previous described in detail in Chapter II. The IMV solutions were buffer exchanged for PBS using a 1-step 3 M sucrose cushion. Briefly, the IMV solution was diluted with PBS and then added over the sucrose cushion and centrifuged at 13,200 rpm for 1 hr. The IMV band was removed, mixed with PBS and centrifuged over a sucrose cushion, 4 rounds total. The IMV solutions were diluted with glycerol (40% v/v), aliquoted into 200 μL aliquots and flash frozen with liquid nitrogen.

Labeling of Inner Membrane Vesicles. This procedure is detailed in Chapter II. The IMVs used in this report were labeled by mixing 400 μL of IMV solution with 50 μL of 1 M bicarbonate buffer (pH 8.5) and then reacting with 0.5 mg of Alexa Fluor 594 carboxylic, acid succimidyl ester suspended in 25 μL of 200 proof ethanol. The reaction mixtures were vortexed vigorously at room temperature for 1 min every 10 min for an hour, and then stored at 4°C overnight. The unconjugated dye was removed using the sucrose cushion procedure described in the previous section for preparing the IMVs, except that TBS was used and the process was repeated until the solution over the pelleted IMV band was colorless.

Preparation of Hybrid Vesicles. The optical density at 280 nm of the IMV solution was measured and adjusted by either dilution or concentration to produce a stock with an O.D. at 280 nm of 4. This solution was then mixed 1:5 by volume with 0.5% PEG5Kce, 99.5% POPC. After vortexing, the solution was bath sonicated at 25°C for 2 hr. The sample was removed from the sonicator, vortexed every 20 min, shaken to the bottom of the tube, and then returned to the sonicator. Samples were usually 50 μL total volume.

Preparation of PDMS Wells and Stamps. Polydimethylsiloxane (PDMS) was used to create wells for containing the SLBs. Sheets of uniform thickness (150±15 μm) were created by polymerizing the PDMS between two annealed/silanized glass slides spaced apart with coverslips (No. 1.5). These sheets were cut to the dimensions of the glass coverslips and a channel of ~2.2 cm by 4 mm was cut into their centers. These wells were cleaned and applied to the glass substrate and all bubbles between the PDMS and glass were removed via mechanical pressure. PDMS stamps were created in a similar manner, but the polymer films

were ~2 mm thick. The stamps were cut to have a footprint of ~3 mm by 400 μm, then rinsed (3x) with nanopure water and ethanol, blown dry with nitrogen, oxygen plasma cleaned for 1 min bottom-side-up, followed by placement in the desired location within the PDMS well. Plasma cleaning was achieved using a PDC-32G from Harrick Scientific (Ossining, NY).

Preparation of the Double Cushioned Heterogeneous Supported Lipid Bilayers. Once the PDMS well and stamp were positioned on the coverslip, 30 μL of 0.01 mg/mL BSA in TBS was added to the well and allowed to incubate for 20 min. After extensively rinsing the BSA solution from the well using TBS, 30 μL of the primary vesicle solution (20% Chol, 0.5% PEG5Kce, 79.5% POPC) was used to create the separation SLB via a 20 min incubation. Then the well was thoroughly rinsed again with TBS and the stamp removed. Next, 30 μL of 0.01 mg/mL BSA in TBS was added again to create a passivation layer in the stamp's previous location. This time the incubation was for 15 min. If a longer incubation time is used, the separation bilayer will invade the stamp region and eventually fill it. However, it is believed a bit of encroachment by the separation bilayer aids in making a continuous SLB between the two bilayers in the system. Once the BSA was rinsed from the system again, the secondary vesicle solution was added along with 10 μL of 4 M NaCl. NaCl screens the negative charge repulsion between the analytes and substrate, facilitating the vesicle fusion process.[59,82] The vesicle solutions were allowed to incubate for 15 min before thoroughly rinsing. This process created a discrete secondary SLB (the origin) inside a larger primary SLB (separation region), as illustrated in Figure 13.

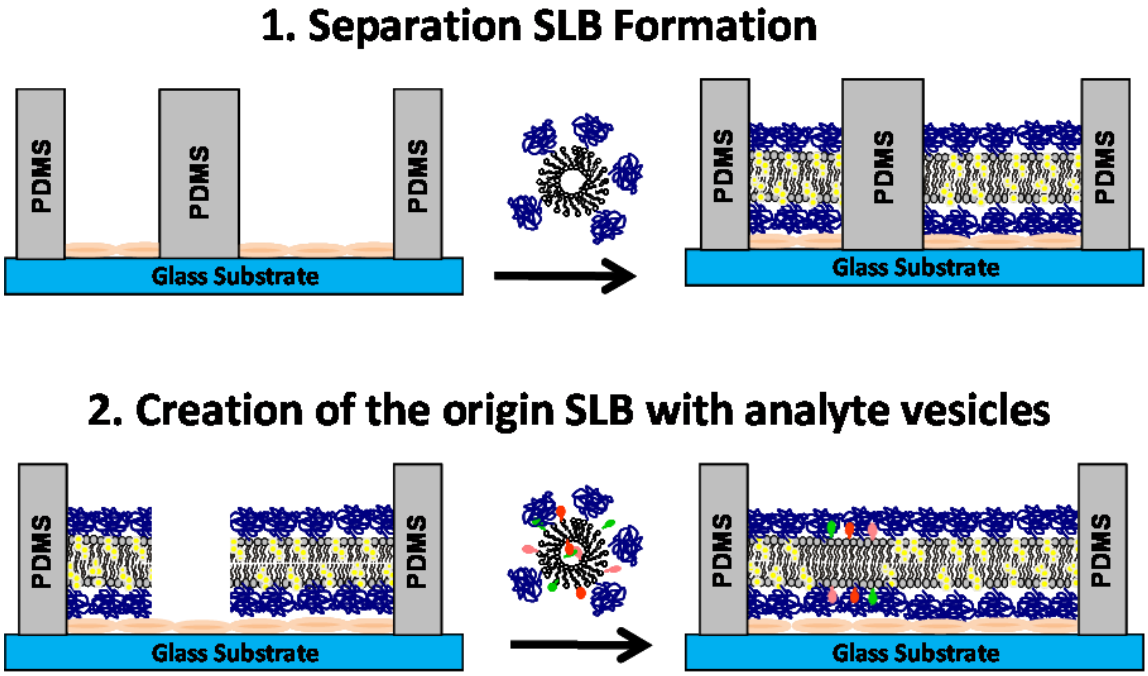

Figure 13. Schematic representation of the stamp method used for double cushioned heterogeneous SLB preparation. First, BSA passivation layer was created in the PDMS well around the stamp. Second, the separation SLB was formed in the PDMS well with the PDMS stamp in place. After rinsing away excess unfused vesicles, the PDMS stamp was removed and the substrate beneath the stamp was passivated with BSA. Finally, analyte vesicle solution was added to produce a continuous double cushioned heterogeneous SLB. Yellow, peach, and blue molecules in the bilayer represent cholesterol, BSA, and PEG, respectively. Red, pink, and green molecules represent fluorescently labeled analytes in the bilayer.

Measuring Diffusion and Mobility. Diffusion and mobility within a SLB is most commonly measured with the technique known as Fluorescence Recovery After Photo-bleaching (FRAP).[83,84] A 2.5 W mixed gas argon/krypton ion laser (Stabilite 2018, Spectra Physics) was used to irradiate the sample with 568 nm light at 50 mW of power for 3 s. A 13 μm fwhm bleach spot was produced by focusing the light onto the sample through a 10X objective on an inverted epifluorescence Nikon microscope. The fluorescence recovery was recorded as a function of time using MetaMorph Software (Universal Imaging), after background subtraction and intensity normalization. The fluorescence recovery data were fit to a double exponential rise to maximum equation (Eq. 1) in order to extract the contributions to the total recovery of both a fast moving (i.e., lipid) component and slower moving (i.e., protein) component present within the sample.

$$y = a(1 - e^{-bx}) + c(1 - e^{-dx}) \quad (1)$$

In this equation, *a* and *c* are weighting factors for the contributions of each of the two species. When the data has an R^2 fit of 0.97 or higher to Equation 1, these two values accurately add up to the predicted maximum value of the normalized fluorescence, *y*. These weighting values were used to calculate the percentage contribution to the total recovery. Herein, the values of *b* and *d* are the kinetic constants k_1 and k_2, respectively. The kinetic constants are used to calculate the half-times of recovery ($t_{1/2}$) via Eq. 2.

$$t_{1/2} = ln2/k \quad (2)$$

Using these half-time recovery values, fwhm of the Gaussian profile of the focused laser beam (*w*), and a correction factor related to beam geometry and bleach time (γ_D), equation 3 could be used to calculate the lateral diffusion coefficient of each species.[83]

$$D = \left(\frac{w^2}{4t_{\frac{1}{2}}}\right)\gamma_D \quad (3)$$

In these experiments w = 13 μm and γD = 0.88.

Supported Lipid Bilayer Electrophoresis. The heterogeneous SLB was coupled to an electrophoretic flow cell device, described previously in Chapter III.[23] Briefly, the device allows electrophoresis to occur under constant buffering conditions while removing the products of electrolysis and mitigating joule heating. These experiments were performed under a constant flow of 1 mM Tris buffer (no NaCl, pH 7.5, ~1.5 mL/min flow rate) for usually 20 min at 600 V (average current ~200 μA). No measurable pH variations were observed under these conditions. Electrophoretic separation of the Alexa Fluor 594 labeled IMV material was monitored in real-time using a 4X objective on an upright epifluorescence Nikon microscope.

Visualizing the IMV Components Post-separation. After electrophoresis, the device was inverted and the clamps holding it together were removed. The device with coverslip and glass support was submerged into a bath of running buffer. The buffer flow dislodged the coverslip from the Teflon body. The coverslip with intact PDMS well was then brought out of the bath under a gentle stream of TBS from a squirt bottle. The well was then thoroughly rinsed with TBS. The staining agent of interest was then added and allowed to incubate at room temperature.

For antibody labeling, 1 μL of primary (1°) antibody was added and allowed to incubate for 30 min. After extensively rinsing the sample with TBS, 1 μL of secondary

(2°) antibody was added and allowed to incubate for 30 min. The 2° was labeled with Alexa Fluor 488 and was specific for antibodies (i.e., IgG) from the organism that was used to produce the 1°. Once the all unbound antibodies had been removed via rinsing the samples with TBS, the samples were imaged using an upright epifluorescence Nikon microscope equipped with MetaMorph imaging software. Images were taken using both the 594 nm and 488 nm filter sets for comparison of the Alexa Fluor 594 dye-labeled IMV components and the Alexa Fluor 488 dye-labeled antibodies. Line scans were used to aid in the interpretation of the micrographs. The line scans in this report were corrected for background and vignetting.

In order to prove that the samples were free of DNA or RNA, 1 uL of 1 mM stock Yo-Pro reagent from Invitrogen (Carlsbad, CA) was added to the SLB post electrophoresis and allowed to incubate for 30 min. The free dye was washed away and the sample was observed using the appropriate filter set on the fluorescent microscope. No staining of the SLB was observed. Invitrogen technical support confirmed that this procedure should label DNA/RNA immobilized on a surface, but there are no reports to date of this reagent being used in such a manner.

Results and Discussion

Two types of *E. coli* MC4100 IMVs were used in this report. One was produced from a knock-out strain (ΔTatABCDE), which had the Twin-Arginine Translocase proteins TatA, TatB, TatC, TatD, and TatE deleted. The other was produced from a strain with TatA,

TatB, and TatC overexpressed. Unless otherwise noted, the data discussed herein were produced using IMVs derived from the overexpressed strain.

Fluorescently Labeling IMV Components. The Alexa Fluor 594 carboxylic acid, succimidyl ester dye used reacts with free amines (mostly primary amines and to a lesser extent secondary amines). Thus, normally lysine residues and N-termini are the species labeled within proteins. However, phosphatidylethanolamine (PE), which bears a primary amine headgroup, is the most abundant lipid in the inner membrane of E. coli.[85] With a pKa of ~7.5 (vs. ~10.5 for lysine) the PE should always be preferentially labeled over the lysines present. As the FRAP and electrophoresis data below show this is indeed the case.

Creating IMV-Derived SLBs with Lateral Mobility. The IMVs alone do not create mobile membranes, in that there is no observed recovery in experiments. It is believed that IMVs simply adsorb to the surface, but do not fuse to become a bilayer due to the complexity of their lipid composition and high protein content.[82,86,87] Mobile bilayers were created by mixing the IMVs with 0.5%PEG5Kce_99.5%POPC vesicles via sonication. This concentration of PEG5Kce was chosen based on previous work utilizing the double cushion architecture.[15] Indeed, the use of PEG5Kce at the mushroom-to-brush transition (0.5 mol %) provides the optimal surface density to produce the greatest distance between the glass substrate and bilayer (4.8 nm) without introducing surface pressures from over-crowding the membrane surface, which would hinder lateral

diffusion.[48] The ratio of IMV to PEG5Kce_POPC vesicles was found to be optimal when mixing an IMV solution with an O.D. at 280 nm of 4 with the 1 mg/mL PEG5Kce_POPC vesicles at a 1 to 4 (v/v), respectively. Through various formulations it was observed that if the fraction of IMVs is raised, then the bilayers become increasingly less mobile and if the fraction is too low, then the membrane components become too dilute to visualize.

The combination of the double cushion architecture and optimal IMV to PEG5Kce_POPC ratio can produce SLBs with up to ~80% mobile fraction, an unprecedented measurement considering the fact that these membranes are produced from actual native membranes.[79-81] Figure 14 shows micrographs of an SLB before and after recovery, as well as, the measured FRAP curve. It is worth noting how pristine and homogenous the IMV derived SLBs are in these micrographs and the quality of the FRAP curve it generated. All FRAP data presented herein were fit with a double exponential rise to max function in order to calculate the contributions of both the fast moving lipid fraction and slower moving protein fraction. This is a valid approach since the fluorescence being recovered is from both labeled proteins and lipids.

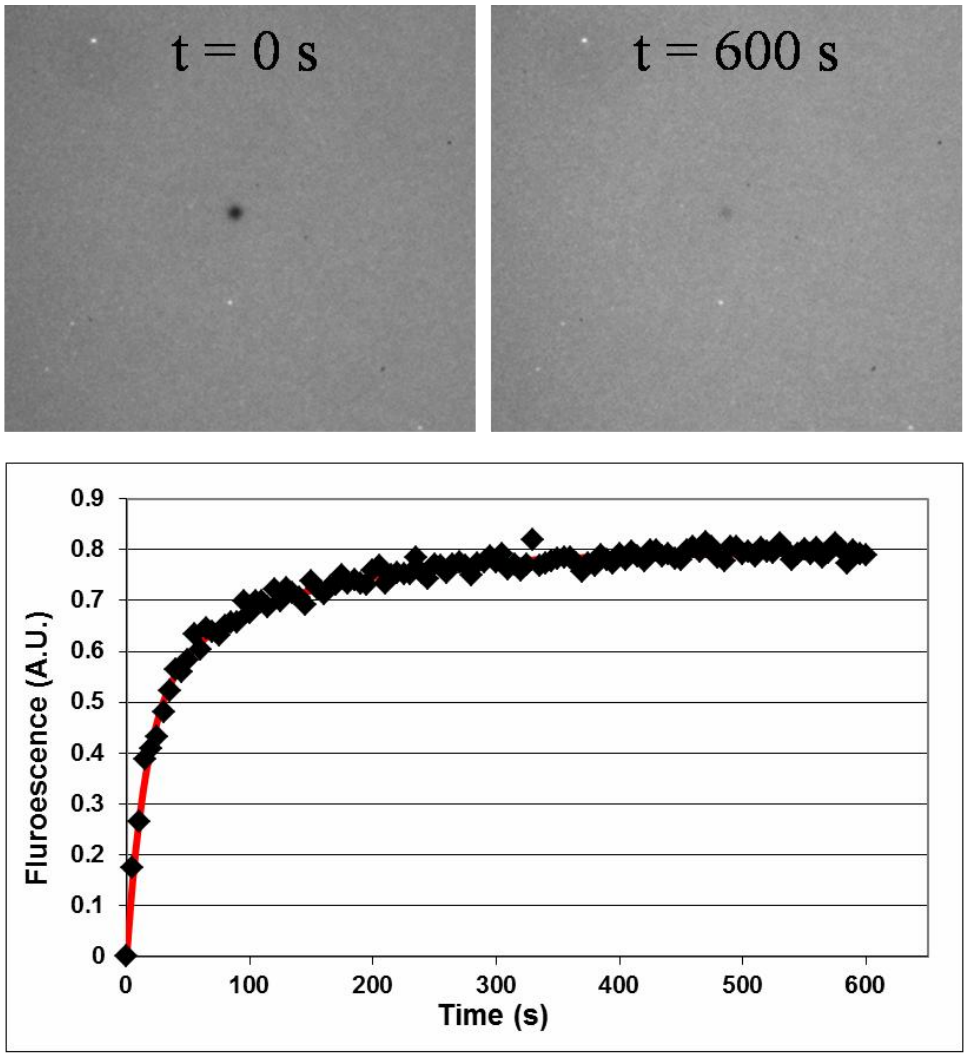

Figure 14. FRAP curve from a double cushioned SLB derived from *E. coli* IMVs labeled with Alexa Fluor 594. The passivation cushion was made by incubation with 0.01 mg/mL BSA. The black diamonds are the raw data and the red line is the double exponential rise to max fit, which had an R^2 = 0.99. Micrographs of the double cushioned SLB before (t = 0 s) and after (t = 600 s) recovery are shown above the graph.

Table 2 compares FRAP data attained as a function of the BSA concentration used in creating the BSA portion of the double cushion architecture (i.e., the passivation layer). It was observed that the range of 0-0.1 mg/mL produced virtually no variation on the percent recovery, diffusion coefficients, or percent contributions from either protein or lipid. This outcome was also observed in our previous double cushion work.[19] Additionally, it is important to note that the diffusion coefficients calculated nicely match previous reported values for both lipids and transmembrane proteins.[16,88] When 0.5 mg/mL BSA was used to create a passivation layer, it adversely affected the percent recovery and the diffusion of both proteins and lipids within the SLB. It is interesting to note that the relative contributions of the proteins and lipids to the mobility remained the same. Indeed, both species had a ~40% smaller diffusion coefficient. In our previous work, the diffusion coefficient of Texas Red DHPE, a lipid, dropped to zero when 0.5 mg/mL BSA was used passivate the surface.[15] It was suggested that an increase in surface roughness was to blame. If so, then perhaps the disparity in our results is caused by the endogenous hopanoids (prokaryotic version of sterols) from the IMVs, which would produce a stronger and more rigid SLB tolerable to the increased surface roughness.

Table 2. Diffusion Characteristics on Various BSA Cushions

[BSA] (mg/mL)	% Recovery	Fast D ($\mu m^2/s$)	Slow D ($\mu m^2/s$)	%Fast	%Slow	Rsqr
0	79.3±2.1	3.5±0.3	0.41±0.13	64±3	36±3	0.97±0.01
0.01	78.3±1.2	3.3±0.1	0.41±0.05	66±1	34±1	0.98±0.01
0.1	78.3±1.4	3.2±0.1	0.42±0.05	63±6	37±6	0.99±0.00
0.5	67.3±1.5	1.9±0.3	0.25±0.05	65±2	35±2	0.99±0.01

Separation of IMV Material within a SLB. The highly mobile double cushion SLBs discussed thus far were integrated into the heterogeneous SLB procedure described in Chapter IV as diagrammed in Figure 13. The samples were then mounted to the flow cell described in Chapter III, as previously described. All electrophoresis data herein is oriented with the cathode on the left and the anode on the right.

Figure 15 shows the Alexa Fluor 594 labeled IMV material moving towards the anode and separating into three bands within 20 minutes. The fastest band makes up ~2% of the total fluorescently labeled material and has an apparent electrophoretic mobility of 0.34±0.01 (μm/min)/(V/cm). The intermediate band and slowest bands each make up ~10% and ~70% of the fluorescent material, respectively. Their apparent electrophoretic mobilities are 0.11±0.00 and 0.057±0.002 (μm/min)/(V/cm), respectively. For reference, the electrophoretic mobility of Texas Red-DHPE para- and ortho- isomers in this system were measured to be 0.11 and 0.066 (μm/min)/(V/cm), respectively. The Alexa Fluor 594 dye used comes as a mixture of two isomers (meta- and para-) as well, thus it is postulated that these two bands represent the PE lipid components of the IMV that were labeled with the different isomers. Due to the structural homology between Texas Red and Alexa Fluor 594, it is also believed that both would produce dye-labeled PE species with the same net charges, supporting the similarity in electrophoretic mobilities. Additionally, the data in Figure 15 supports the FRAP measurement of a ~20% immobile fraction.

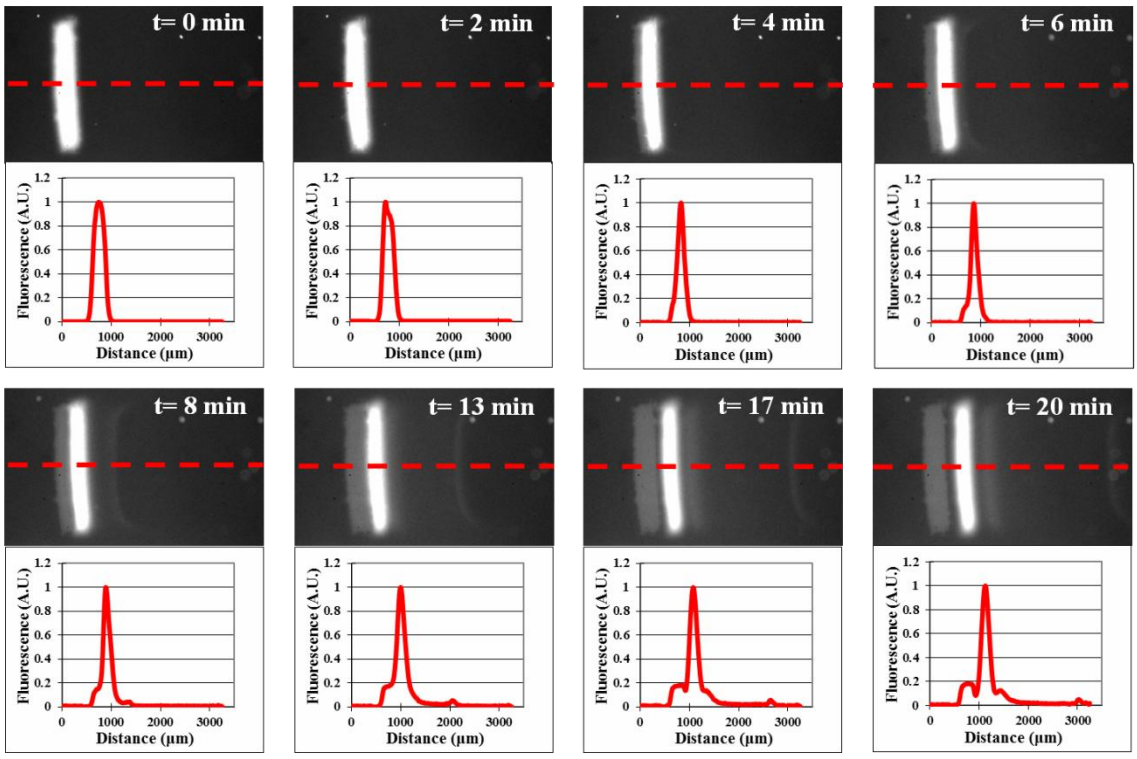

Figure 15. Time lapsed micrographs and associated line scans of the electrophoretic separation of a heterogeneous double cushioned SLB derived from Alexa Fluor 594 labeled *E. coli* IMVs. The line scans associated with each micrograph detail the intensity profile along the dotted line present in each micrograph. Micrographs and line scans are oriented with the cathode on the right and the anode on the left. The x-axis of each line scan details the width of both the origin and each of the separated bands.

In order to visualize the proteins present in the SLB post-electrophoresis, a pseudo-Western blotting procedure was developed, which will be referred to as immunostaining for the rest of this report. The primary antibody was a polyclonal mixture against the overexpressed Twin-Arginine Translocase protein TatB, which was contained in rabbit serum and produced by a collaborator. The secondary antibody was a commercially available goat anti-rabbit IgG polyclonal conjugated with Alexa Fluor 488 dye.

Figure 16A is the micrograph of the SLB post separation and subsequent to immunostaining using the 594 nm filter set. It is the same sample as shown in Figure 15, but after the 1 hr immunostaining procedure, and hence, the peaks have broadened and the resolution between the slow and intermediate peaks has decreased. Indeed, upon observation 24 hr later, the slow and intermediate peaks are substantially more diffuse (data not shown). This observation is in contrast to the antibody-labeled bands, which experience little to no diffusion, supporting the conclusion that the slow and intermediate bands are in fact lipid populations. Previous reports have suggested that the pseudo-Western blot style antibody labeling of proteins within a SLB makes them immobile.[26]

Figure 16B is the same sample viewed at the same time as 16A, but using the 488 nm filter set. The bands observed with the 488 nm filter are proteins which have been nonspecifically labeled via the immunostaining procedure. Figure 16C shows the line scans of both 16A and 16B taken along the same vector, which were overlaid for comparison. Eight mobile protein populations, five anodic and three cathodic, are easily observed with the 488 nm filter set. This overlay shows that the fastest moving anodic

band seen in the 594 nm channel is actually protein. Additionally, that band had the highest concentration of the proteins present, which explains why it was the only protein visible in the 594 channel. The other proteins that may have been dye labeled as well simply do not have large enough populations to be observed in the 594 channel. Due to the lack of base line resolution, quantitation of the relative populations within each band was not pursued. Additionally, it is believed that the lack of base line resolution draws from the fact that there is a very large population of proteins that are moving in the anodic direction, thus producing a large background signal in that region. Perhaps tuning of the separation SLB in future experiments would provide increased resolution of these bands, as has been previously reported.[22] It can be estimated however that ~85% of the 488 nm signal in the line scan is present outside of the origin. In other words, ~85% of the proteins labeled via immunostaining are mobile.

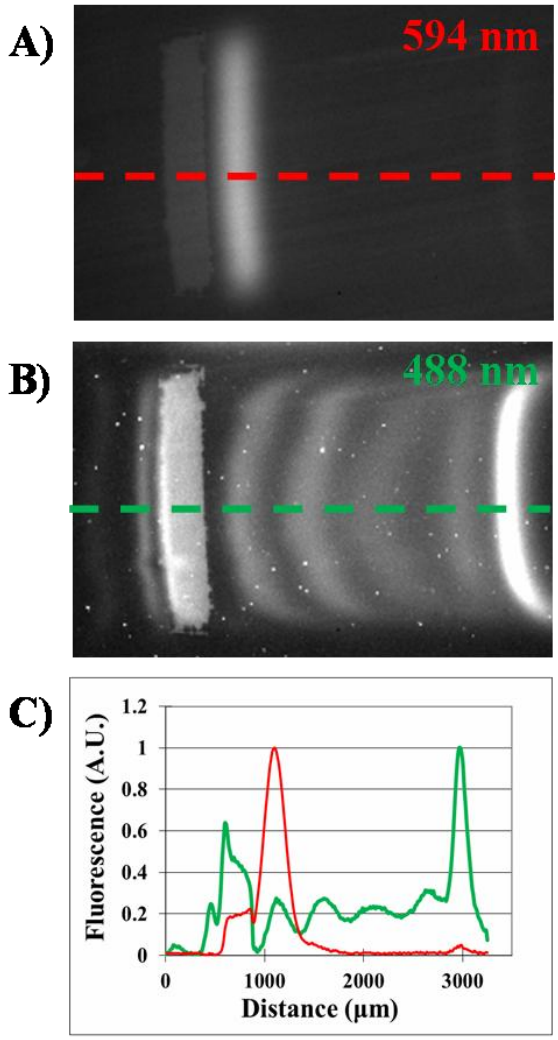

Figure 16. Micrographs and associated line scans for comparison of the Alexa Fluor 594 dye labeled and Alexa Fluor 488 antibody labeled IMV components post-electrophoresis. A) Micrograph of SLB using the 594 nm filter set. B) Micrograph of the SLB using the 488 nm filter set. C) Overlaid line scans detailing the intensity profiles along the dotted lines shown in each corresponding micrograph. The red line is for the 594 nm micrograph and the green line is for the 488 nm micrograph. The widths of the peaks can be evaluated using the x-axis of the line scan.

It has been reported that the distribution of isoelectric points in the *E. coli* proteome has a bimodial nature with maxima at ~5.8 and ~9.3, with virtually no species at 7.5. While membrane proteins are said to have more alkaline isoelectric points in general, there are also many exceptions.[89] The TatABC proteins, for example, each have isoelectric points between pH 5-6.[90] Thus electrophoresis experiments performed at pH 7.5 should expect to produce proteins moving both cathodically and anodically, as observed. Additional experiments with electrophoresis performed at various pHs would provide interesting insight.

In an attempt to accurately identify the protein bands, several other primary antibodies as well as the *E. coli* TatABC deletion strain were utilized. Figure 17 shows a series of micrographs taken after electrophoresis and subsequent immunostaining with the 488 nm filter set and their associated line scans. Figure 17A shows the *E. coli* TatABC deletion strain after immunostaining with the same anti-TatB antibody used in Figure 16B. If the antibody was truly specific to only TatB, no immunostaining of the SLB would be observed because no TatB is present. While the micrograph appears relatively weak, the line scan clearly shows there is a similar pattern to that observed in figure 16B. The relative intensities of the protein populations are the same. Due to the limited field of view, the cathodic bands were not shown; however, they were present. In order to rule out that the staining pattern was not being produced by the non-specific adsorption of the secondary antibody, a sample was stained with only secondary antibody. No fluorescence was observed within the separation region (data not shown). Figures 17B-D were all produced using the TatABC overexpressed strain used in Figure

16B, only the primary antibody used during immunostaining was different. Figure 17B shows the pattern produced by using an anti-TatA primary antibody. The origin stains brighter than the protein peaks do with this antibody; however, the pattern is still present.

Next the source of the anti-TatA and anti-TatB antibodies was tested. Both were contained in serum and obtained from Dr. Musser's lab, so another antibody was obtained that was produced with the same procedure, anti-pre-SufI. Pre-SufI is a soluble protein that binds to the Tat machinery, but is not present in the IMVs received from our collaborators. Figure 17C shows again another antibody that should not bind to the proteins present does so in the same pattern. This result suggests that there is a contaminant in all the antibody serum solutions. Another control experiment was run in which commercially available anti-6XHis-tag antibody was used as the primary antibody and no fluorescence was observed in the staining region (data not shown).

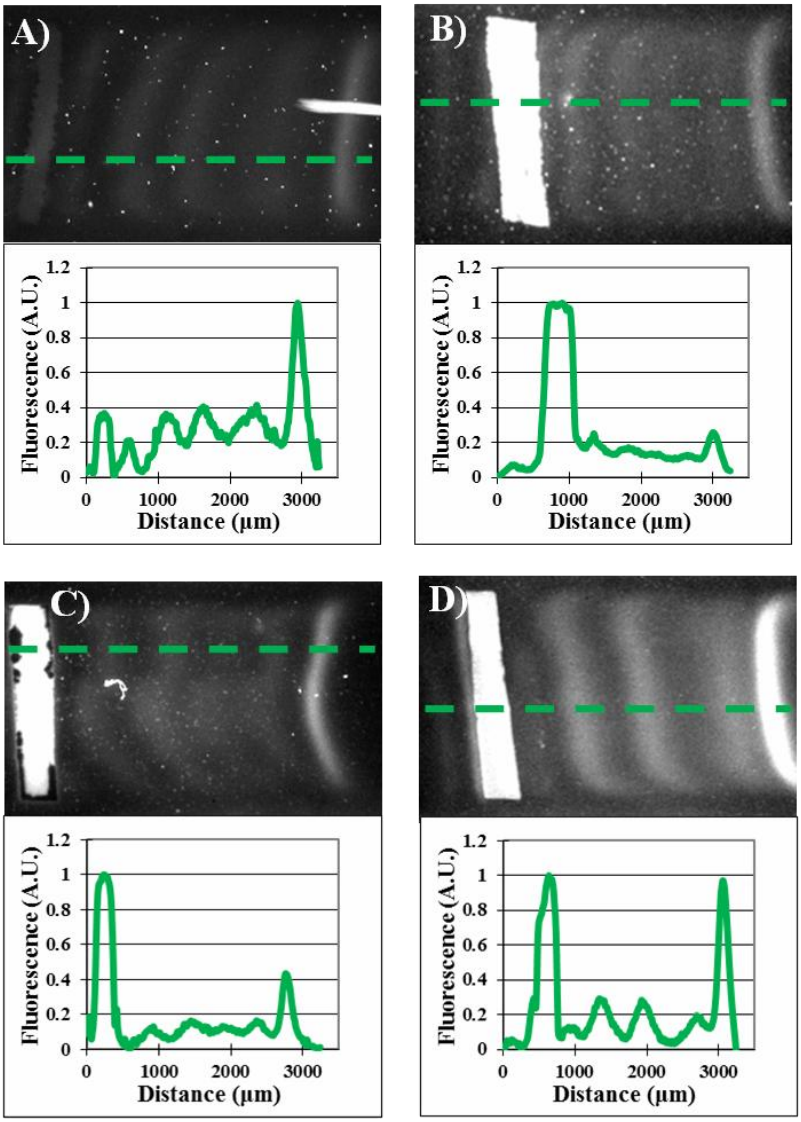

Figure 17. Micrographs and associated line scans from a variety of primary antibodies. Variations in the IMVs and primary antibodies used for immunostaining were utilized in an attempt to identify the protein bands previously observed in Figure 16. A) Anti-TatB stained separation of a TatABC deletion strain of E. coli. B) Anti-TatA stained separation of a TatABC overexpressed strain of E. coli. C) Anti-pre-SufI stained separation of a TatABC overexpressed strain of E. coli. D) Purified anti-TatB stained separation of a TatABC overexpressed strain of E. coli. The associated line scan of each micrograph details the intensity profile along the doted, respectively. Peak dimensions can be inferred from the x-axis of each line scan.

In an attempt to remove the contaminant from serum, a Melon Gel IgG Purification kit from Thermo Scientific was used, which removes most protein found in serum as well as other contaminants from cell culture while allowing IgG to elute freely. Figure 17D shows the results of using anti-TatB antibodies purified with this kit. Aside from enhanced staining of the origin, the same pattern was seen as compared to the unpurified stock used for Figure 16B. Since it is clear that the antibodies produced from this source cannot yield specific staining data due to contaminants, commercially available antibodies against some of the more abundant *E. coli* membrane proteins will be the next strategy for identifying these mobile protein bands.

Conclusion

This report illustrates the long awaited methodology of producing highly mobile native membranes on planar supports. The mixing of dye labeled IMVs with PEGylated lipids was shown to produce highly homogenous SLBs with ~80% of the dye labeled species being mobile, of which ~35% demonstrated a diffusion coefficient on the order of transmembrane protein. The use of double cushioned heterogeneous SLB electrophoresis successfully produced eight mobile populations of membrane proteins from a single patterned patch. Additionally, two dye-labeled lipid populations were separated from the same patch. The ability to dismount the sample from the electrophoresis device for further analysis, as demonstrated by the subsequent antibody staining procedures, proves the utility of this technique to pre-fractionate complex native membrane mixtures for further analysis. While the identities of the separated bands has

yet to be solved, the nonspecific staining observed does supply the proof of principle that the methodologies described herein have the potential to significantly impact the membrane research community.

CHAPTER VI

CONCLUSION

The use of SLBs to study the composition and characteristics of cell membranes is developing field and this dissertation chronicles some of the newly developed tools for such studies. Herein we have described the development of a flow cell for the manipulation of charged membrane components, a new technique for the label-free visualization of SLB components, and a methodology for the patterning and subsequent fractionation of native membranes derived from IMVs of *E. coli*.

In Chapter III, a newly designed flow cell was proven to strictly control the pH and ionic strength above a SLB during electrophoresis. This control allowed for the modulation of membrane-bound streptavidin's electrophoretic mobility as a function of pH, the presence or absence of a PEG cushion support and the ionic strength. Indeed, the tuning of these parameters allowed for the migration of streptavidin to be increased, decreased and even change direction. In all of these cases TR-DHPE served as an internal reference compound that was relatively insensitive to these variables. These results suggest the potential to precisely control the movement of membrane bound species in supported lipid bilayers.

Chapter IV introduces the capability to couple SLB separations and MALDI-MS imaging technologies in order to develop a new analytical platform for the separation and detection of membrane components from vesicles containing complex analyte mixtures. Herein the separation of five membrane components using SLB

electrophoresis was visualized using MALDI-MS imaging. The label-free nature of MALDI-MS imaging allowed for the visualization of three unadulterated naturally occurring membrane species, two of which are biologically relevant cell surface receptors, post-electrophoretic separation. While Chapter IV only shows the separation and subsequent imaging of lipid species, the potential for this technology to be extended to examine membrane proteins, with the eventual goal of separating and imaging components from native membranes, is being examined.

Chapter V describes the methods needed to produce highly mobile native membranes on planar supports. The mobility of these *E. coli* IMV-derived SLBs was probed through the use of FRAP techniques and free amine labeling of the IMV material. Indeed, the mixing of dye labeled IMVs with PEGylated lipids was shown to produce highly homogenous SLBs with ~80% of the dye labeled species being mobile, of which ~35% displayed the characteristic diffusion coefficient of membrane proteins. Additionally, the use of double-cushioned heterogeneous SLB electrophoresis successfully produced 8 mobile populations of membrane proteins from a single patterned patch. These populations were identified as proteins and visualized through the use of a pseudo-Western blot antibody staining procedure. These advances will not only allow for the generation of large planar native membrane samples for biophysical analysis, but also show promise as a new analytical technique for membrane protein separations.

REFERENCES

(1) Han, X. L.; Gross, R. W. *Mass Spectrom Rev* **2005**, *24*, 367.

(2) Santoni, V.; Molloy, M.; Rabilloud, T. *Electrophoresis* **2000**, *21*, 1054.

(3) Gorg, A.; Weiss, W.; Dunn, M. J. *Proteomics* **2004**, *4*, 3665.

(4) Wu, C. C.; MacCoss, M. J.; Howell, K. E.; Yates, J. R. *Nat Biotechnol* **2003**, *21*, 532.

(5) Lundstrom, K. *Cell Mol Life Sci* **2006**, *63*, 2597.

(6) Brian, A. A.; Mcconnell, H. M. *P Natl Acad Sci-Biol* **1984**, *81*, 6159.

(7) Tamm, L. K.; Mcconnell, H. M. *Biophys J* **1985**, *47*, 105.

(8) Sackmann, E. *Science* **1996**, *271*, 43.

(9) Castellana, E. T.; Cremer, P. S. *Surf Sci Rep* **2006**, *61*, 429.

(10) Kiessling, V.; Domanska, M. K.; Murray, D.; Wan, C.; Tamm, L. K.; Begley, T. P. In *Wiley Encyclopedia of Chemical Biology*; John Wiley & Sons, Inc.: 2007. DOI: 10.1002/9780470048672.wecb663

(11) Salafsky, J.; Groves, J. T.; Boxer, S. G. *Biochemistry-Us* **1996**, *35*, 14773.

(12) Davis, R. W.; Flores, A.; Barrick, T. A.; Cox, J. M.; Brozik, S. M.; Lopez, G. P.; Brozik, J. A. *Langmuir* **2007**, *23*, 3864.

(13) Goennenwein, S.; Tanaka, M.; Hu, B.; Moroder, L.; Sackmann, E. *Biophys J* **2003**, *85*, 646.

(14) Smith, E. A.; Coym, J. W.; Cowell, S. M.; Tokimoto, T.; Hruby, V. J.; Yamamura, H. I.; Wirth, M. J. *Langmuir* **2005**, *21*, 9644.

(15) Diaz, A. J.; Albertorio, F.; Daniel, S.; Cremer, P. S. *Langmuir* **2008**, *24*, 6820.

(16) Roder, F.; Waichman, S.; Paterok, D.; Schubert, R.; Richter, C.; Liedberg, B.; Piehler, J. *Anal Chem* **2011**, *83*, 6792.

(17) Tanaka, M.; Sackmann, E. *Nature* **2005**, *437*, 656.

(18) Stelzle, M.; Miehlich, R.; Sackmann, E. *Biophys J* **1992**, *63*, 1346.

(19) Groves, J. T.; Boxer, S. G. *Biophys J* **1995**, *69*, 1972.

(20) Groves, J. T.; Wulfing, C.; Boxer, S. G. *Biophys J* **1996**, *71*, 2716.

(21) Cremer, P. S.; Groves, J. T.; Kung, L. A.; Boxer, S. G. *Langmuir* **1999**, *15*, 3893.

(22) Daniel, S.; Diaz, A. J.; Martinez, K. M.; Bench, B. J.; Albertorio, F.; Cremer, P. S. *J Am Chem Soc* **2007**, *129*, 8072.

(23) Monson, C. F.; Pace, H. P.; Liu, C. M.; Cremer, P. S. *Anal Chem* **2011**, *83*, 2090.

(24) Burns, A. R. *Langmuir* **2003**, *19*, 8358.

(25) Wagner, M. L.; Tamm, L. K. *Biophys J* **2000**, *79*, 1400.

(26) Wagner, M. L.; Tamm, L. K. *Biophys J* **2001**, *81*, 266.

(27) Purrucker, O.; Fortig, A.; Jordan, R.; Tanaka, M. *Chemphyschem* **2004**, *5*, 327.

(28) Purrucker, O.; Fortig, A.; Jordan, R.; Sackmann, E.; Tanaka, M. *Phys Rev Lett* **2007**, *98*.

(29) Jonsson, P.; Beech, J. P.; Tegenfeldt, J. O.; Hook, F. *J Am Chem Soc* **2009**, *131*, 5294.

(30) Neumann, J.; Hennig, M.; Wixforth, A.; Manus, S.; Radler, J. O.; Schneider, M. F. *Nano Lett* **2010**, *10*, 2903.

(31) Reviakine, I.; Brisson, A. *Langmuir* **2001**, *17*, 8293.

(32) Grogan, M. J.; Kaizuka, Y.; Conrad, R. M.; Groves, J. T.; Bertozzi, C. R. *J Am Chem Soc* **2005**, *127*, 14383.

(33) Tanaka, M.; Hermann, J.; Haase, I.; Fischer, M.; Boxer, S. G. *Langmuir* **2007**, *23*, 5638.

(34) Han, X. J.; Cheetham, M. R.; Sheikh, K.; Olmsted, P. D.; Bushby, R. J.; Evans, S. D. *Integr Biol* **2009**, *1*, 205.

(35) Braun, R. J.; Kinkl, N.; Beer, M.; Ueffing, M. *Anal Bioanal Chem* **2007**, *389*, 1033.

(36) *Electrophoresis: Theory, Methods, and Applications*; Academic Press: New York, 1967; Vol. 2.

(37) Yang, T. L.; Jung, S. Y.; Mao, H. B.; Cremer, P. S. *Anal Chem* **2001**, *73*, 165.

(38) Hope, M. J.; Bally, M. B.; Webb, G.; Cullis, P. R. *Biochim Biophys Acta* **1985**, *812*, 55.

(39) Mayer, L. D.; Hope, M. J.; Cullis, P. R. *Biochim Biophys Acta* **1986**, *858*, 161.

(40) Groves, J. T.; Ulman, N.; Cremer, P. S.; Boxer, S. G. *Langmuir* **1998**, *14*, 3347.

(41) Molecular Probes. Alexa Fluor 488 Protein Labeling Kit Instructions

(42) Fonslow, B. R.; Barocas, V. H.; Bowser, M. T. *Anal Chem* **2006**, *78*, 5369.

(43) Bayer, E. A.; Benhur, H.; Hiller, Y.; Wilchek, M. *Biochem J* **1989**, *259*, 369.

(44) Sivasankar, S.; Subramaniam, S.; Leckband, D. *P Natl Acad Sci USA* **1998**, *95*, 12961.

(45) Craig, D. B.; Dovichi, N. J. *Anal Chem* **1998**, *70*, 2493.

(46) Sano, T.; Cantor, C. R. *P Natl Acad Sci USA* **1990**, *87*, 142.

(47) Kiessling, V.; Tamm, L. K. *Biophys J* **2003**, *84*, 408.

(48) Marsh, D.; Bartucci, R.; Sportelli, L. *Bba-Biomembranes* **2003**, *1615*, 33.

(49) Israelachvili, J. N. *Intermolecular and surface forces*; 2nd ed.; Academic: San Diego, CA., 1991.

(50) Liu, C. M.; Monson, C. F.; Yang, T. L.; Pace, H.; Cremer, P. S. *Anal Chem* **2011**, *83*, 7876.

(51) Chaurand, P.; Caprioli, R. M. *Electrophoresis* **2002**, *23*, 3125.

(52) Chaurand, P.; Norris, J. L.; Cornett, D. S.; Mobley, J. A.; Caprioli, R. M. *J Proteome Res* **2006**, *5*, 2889.

(53) Heeren, R. M. A.; Smith, D. F.; Stauber, J.; Kukrer-Kaletas, B.; MacAleese, L. *J Am Soc Mass Spectr* **2009**, *20*, 1006.

(54) Kraft, M. L.; Weber, P. K.; Longo, M. L.; Hutcheon, I. D.; Boxer, S. G. *Science* **2006**, *313*, 1948.

(55) Heeren, R. M. A.; McDonnell, L. A.; Amstalden, E.; Luxembourg, S. L.; Altelaar, A. F. M.; Piersma, S. R. *Appl Surf Sci* **2006**, *252*, 6827.

(56) Singh, A. K.; Harrison, S. H.; Schoeniger, J. S. *Anal Chem* **2000**, *72*, 6019.

(57) Imberty, A.; Varrot, A. *Curr Opin Struc Biol* **2008**, *18*, 567.

(58) Lopez, P. H. H.; Schnaar, R. L. *Curr Opin Struc Biol* **2009**, *19*, 549.

(59) Cremer, P. S.; Boxer, S. G. *J Phys Chem B* **1999**, *103*, 2554.

(60) Schwartz, S. A.; Reyzer, M. L.; Caprioli, R. M. *J Mass Spectrom* **2003**, *38*, 699.

(61) Zarei, M.; Bindila, L.; Souady, J.; Dreisewerd, K.; Berkenkamp, S.; Muthing, J.; Peter-Katalinic, J. *J Mass Spectrom* **2008**, *43*, 716.

(62) Skaug, M. J.; Longo, M. L.; Faller, R. *J Phys Chem B* **2009**, *113*, 8758.

(63) Roy, D.; Mukhopadhyay, C. *J Biomol Struct Dyn* **2002**, *19*, 1121.

(64) Righetti, P. G.; Castagna, A.; Antonioli, P.; Boschetti, E. *Electrophoresis* **2005**, *26*, 297.

(65) Kalb, E.; Frey, S.; Tamm, L. K. *Biochim Biophys Acta* **1992**, *1103*, 307.

(66) Hubbard, J. B.; Silin, V.; Plant, A. L. *Biophys Chem* **1998**, *75*, 163.

(67) Tamm, L. K., Shao, Z. In *Biomembrane Structure*; Haris, P. I., Chapman, B., Ed.; IOS Press: Amsterdam, 1998, p 169.

(68) Koenig, B. W.; Gawrisch, K.; Krueger, S.; Orts, W.; Majkrzak, C. F.; Berk, N.; Silverton, J. V. *Biophys J* **1996**, *70*, Wp229.

(69) Thompson, N. L.; Pearce, K. H.; Hsieh, H. V. *Eur Biophys J Biophy* **1993**, *22*, 367.

(70) Yang, T. L.; Baryshnikova, O. K.; Mao, H. B.; Holden, M. A.; Cremer, P. S. *J Am Chem Soc* **2003**, *125*, 4779.

(71) Thompson, N. L.; Drake, A. W.; Chen, L. X.; VandenBroek, W. *Photochem Photobiol* **1997**, *65*, 39.

(72) Cornell, B. A.; BraachMaksvytis, V. L. B.; King, L. G.; Osman, P. D. J.; Raguse, B.; Wieczorek, L.; Pace, R. J. *Nature* **1997**, *387*, 580.

(73) van Oudenaarden, A.; Boxer, S. G. *Science* **1999**, *285*, 1046.

(74) Johnson, J. M.; Ha, T.; Chu, S.; Boxer, S. G. *Biophys J* **2002**, *83*, 3371.

(75) Kim, J.; Kim, G.; Cremer, P. S. *Langmuir* **2001**, *17*, 7255.

(76) Groves, J. T.; Boxer, S. G.; McConnel, H. M. *P Natl Acad Sci USA* **1997**, *94*, 13390.

(77) Olson, D. J.; Johnson, J. M.; Patel, P. D.; Shaqfeh, E. S. G.; Boxer, S. G.; Fuller, G. G. *Langmuir* **2001**, *17*, 7396.

(78) Cheetham, M. R.; Bramble, J. P.; McMillan, D. G. G.; Krzeminski, L.; Han, X.; Johnson, B. R. G.; Bushby, R. J.; Olmsted, P. D.; Jeuken, L. J. C.; Marritt, S. J.; Butt, J. N.; Evans, S. D. *J Am Chem Soc* **2011**, *133*, 6521.

(79) Tanaka, M.; Kaufmann, S.; Nissen, J.; Hochrein, M. *Phys Chem Chem Phys* **2001**, *3*, 4091.

(80) Tanaka, M.; Wong, A. P.; Rehfeldt, F.; Tutus, M.; Kaufmann, S. *J Am Chem Soc* **2004**, *126*, 3257.

(81) Simonsson, L.; Gunnarsson, A.; Wallin, P.; Jonsson, P.; Hook, F. *J Am Chem Soc* **2011**, *133*, 14027.

(82) Nollert, P.; Kiefer, H.; Jahnig, F. *Biophys J* **1995**, *69*, 1447.

(83) Axelrod, D.; Koppel, D. E.; Schlessinger, J.; Elson, E.; Webb, W. W. *Biophys J* **1976**, *16*, 1055.

(84) Jacobson, K.; Derzko, Z.; Wu, E. S.; Hou, Y.; Poste, G. *J Supramol Str Cell* **1976**, *5*, 565.

(85) Vance, D. E.; Vance, J. E. *Biochemistry of lipids, lipoproteins, and membranes*; 4th ed.; Elsevier: Amsterdam ; Boston, 2002.

(86) Graneli, A.; Rydstrom, J.; Kasemo, B.; Hook, F. *Langmuir* **2003**, *19*, 842.

(87) Hamai, C.; Yang, T. L.; Kataoka, S.; Cremer, P. S.; Musser, S. M. *Biophys J* **2006**, *90*, 1241.

(88) Poudel, K. R.; Keller, D. J.; Brozik, J. A. *Langmuir* **2011**, *27*, 320.

(89) Kiraga, J.; Mackiewicz, P.; Mackiewicz, D.; Kowalczuk, M.; Biecek, P.; Polak, N.; Smolarczyk, K.; Dudek, M. R.; Cebrat, S. *Bmc Genomics* **2007**, *8*.

(90) *E. coli* Genome and Proteome Database; http://genprotec.mbl.edu/